A UNIFIED APPROXIMATION OF STOKES-DARCY COUPLED PROBLEM BY A TAYLOR-HOOD METHOD

MARÍA GABRIELA ARMENTANO AND MARÍA LORENA STOCKDALE

Abstract. The goal of this paper is the unified approximation of the two-dimensional Stokes-Darcy coupled problem by a Taylor-Hood method, which uses the space of continuous and piecewise quadratic functions for the velocities and the space of continuous and piecewise linear functions for the pressures. The Taylor-Hood methods are one of the most classical stable finite element approximations for the Stokes problem, however they may not be appropriate for Darcy problem and as a consequence for the coupled problem. In this paper we consider a reformulation of Stokes-Darcy problem which allows us to apply the classical Taylor-Hood elements. An appropriate Fortin operator is constructed in order to show the stability of our method. We show that the method proposed has optimal accuracy and a simple implementation. We also present numerical experiments which confirm the excellent performance of our method.

1. Introduction

The numerical resolution of the Stokes-Darcy coupled problem has been widely studied across multiple articles (see, for example, [4, 5, 22, 23, 27, 28, 30, 31], and the references therein). Some of these articles are devoted to the unified approximation of the coupled problem, i.e., the Stokes and Darcy parts be discretized using the same continuous finite element space. Indeed, in two recent works [4, 5] the authors modified the mixed formulation of the problem in such a way that the new problem has the same solution as the original and, independent of the mesh size, the stability condition for the new Stokes-Darcy problem reduces to the same as the Stokes problem. Based on this approach they approximate the solution by using the MINI-elements for the two-dimensional problem in polygonal domains [4] and in curved domains [5].

In this paper, by using the same modified Stokes-Darcy problem introduced in [4], we solve the Stokes-Darcy problem with a $\mathbf{P}_2P_1$ Taylor-Hood method, i.e., we basically use continuous and piecewise quadratic functions for the velocities and continuous and piecewise linear functions for the pressures.

A standard method for proving the inf-sup condition implying stability of finite element approximations is to construct a Fortin operator. The Taylor-Hood methods, which was introduced by Hood and Taylor in [26], are one of the most classical stable finite element approximations for the Stokes problem, however the construction of a Fortin operator for this family of methods is not easy to perform (even several stability proofs present in the literature use alternative approaches). Therefore, there are multiple works devoted to proof the stability of the method and the construction of the Fortin operator (see [16, 18, 21, 29, 32]

Key words and phrases. Stokes-Darcy problem, Mixed finite elements, Taylor-Hood methods, Stability analysis.

and the references therein) Following the ideas given in the recent work of R. Scott [32] and those given in [4], we construct a Fortin operator for the lowest order Taylor-Hood element in two space dimensions which, under proper conditions, is uniformly bounded both in $\mathbf{H}^1$ norm and allows us to conclude the stability of our approximation method and so optimal accuracy with respect to solution regularity. We also present numerical experiments which confirm the excellent performance of our method.

The rest of the paper is organized as follows. In Section 2 we state the classical Stokes-Darcy coupled problem and we introduce the modified coupled Stokes-Darcy problem. In Section 3 we present the finite element discretization with a Taylor-Hood method and we analyze the stability of the proposed method. Finally, in section 4, we present several numerical examples.

2. Problem Statement

We consider an open, bounded and polygonal domain $\Omega \subset \mathbb{R}^2$ divided into two open subdomains with Lipschitz continuous boundaries Ω_S and Ω_D, where the indices S and D stand for fluid and porous, respectively. We assume that $\overline{\Omega} = \overline{\Omega}_S \cup \overline{\Omega}_D$, $\Omega_S \cap \Omega_D = \emptyset$ and $\overline{\Omega}_S \cap \overline{\Omega}_D = \Gamma_I$ so, Γ_I represents the interface between the fluid and the porous medium. The remaining parts of the boundaries are denoted by $\Gamma_S = \partial\Omega_S \setminus \Gamma_I$ and $\Gamma_D = \partial\Omega_D \setminus \Gamma_I$, as illustrated in Figure 1.

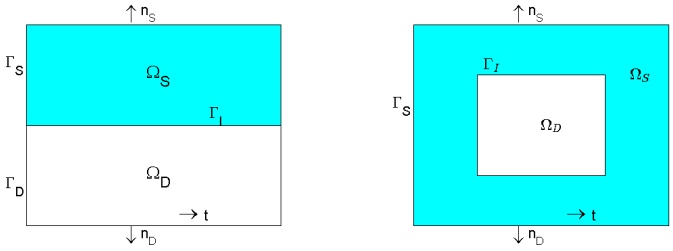

Figure 1. Examples of two-dimensional domains Ω

We denote by $\boldsymbol{n}_S$ the unit outward normal direction on $\partial\Omega_S$ and by $\boldsymbol{n}_D$ the normal direction on $\partial\Omega_D$, oriented outward. On the interface Γ_I, we have $\boldsymbol{n}_S = -\boldsymbol{n}_D$. We also use, as usual, boldface for vector value functions.

The Stokes-Darcy coupled problem describes the motion of an incompressible viscous fluid occupying a region Ω_S which flows across the common interface into a porous medium living in another region Ω_D saturated with the same fluid. The mathematical model of this problem can be defined by two separate groups of equations and a set of coupling terms.

For any function $\mathbf{v}$ defined in Ω, taking into account that its restriction to Ω_S or to Ω_D could play a different mathematical roles, we define $\mathbf{v}_S = \mathbf{v}\,|_{\Omega_S}$ and $\mathbf{v}_D = \mathbf{v}\,|_{\Omega_D}$.

In Ω_S, the fluid motion is governed by the Stokes equations for the velocity $\mathbf{u}_S$ and the pressure p_S:

$$\begin{cases} -\mu\Delta\mathbf{u}_S + \nabla p_S = \mathbf{f}_S, \text{ in } \Omega_S, \\ \text{div } \mathbf{u}_S = 0, \text{ in } \Omega_S, \\ \mathbf{u}_S = 0, \text{ in } \Gamma_S, \end{cases} \tag{2.1}$$

where $\mathbf{f}_S \in (L^2(\Omega_S))^2$ represents the force per unit mass and $\mu > 0$ the viscosity.

In Ω_D, the porous media flow motion is governed by Darcy' law for the velocity $\mathbf{u}_D$ and the pressure p_D:

$$\begin{cases} \frac{\mu}{K}\mathbf{u}_D + \nabla p_D = \mathbf{f}_D, \text{ in } \Omega_D, \\ \text{div } \mathbf{u}_D = g_D, \text{ in } \Omega_D, \\ \mathbf{u}_D \cdot \boldsymbol{n_D} = 0, \text{ in } \Gamma_D, \end{cases} \tag{2.2}$$

where $\mathbf{f}_D \in (L^2(\Omega_D))^2$ represents the force per unit mass, $g_D \in L^2(\Omega_D)$ a source and K denoting the permeability tensor reduced to a positive scalar in the isotropic case considered here.

In Γ_I, we consider the following boundary conditions:

$$\begin{cases} \mathbf{u}_D \cdot \boldsymbol{n}_D + \mathbf{u}_S \cdot \boldsymbol{n}_S = 0, \\ p_S\, \boldsymbol{n}_S - \mu\nabla\mathbf{u}_S\, \boldsymbol{n}_S - p_D\, \boldsymbol{n}_S - \mu\frac{\alpha}{\sqrt{K}}(\mathbf{u}_S \cdot \boldsymbol{t})\, \boldsymbol{t} = 0, \end{cases} \tag{2.3}$$

where, as usual, $\nabla\mathbf{u} = \left(\frac{\partial u_i}{\partial x_j}\right)_{1\le i,j\le 2}$. The first equation represents mass conservation and the second is due to the balance of normal forces and the Beavers-Joseph-Saffman condition, α a parameter determined by experimental evidence and $\boldsymbol{t}$ the tangent vector on Γ_I (we recommend [9] for more details on the interface conditions).

We denote with boldface the spaces consisting of vector value functions. The norms and seminorms in $\mathbf{H}^m(\mathcal{D})$, with m an integer, are denoted by $\|\cdot\|_{m,\mathcal{D}}$ and $|\cdot|_{m,\mathcal{D}}$ respectively and $(\cdot,\cdot)_{\mathcal{D}}$ denotes the inner product in $L^2(\mathcal{D})$ or $\mathbf{L}^2(\mathcal{D})$ for any subdomain $\mathcal{D} \subset \Omega$. The domain subscript is dropped for the case $\mathcal{D} = \Omega$. Let $\mathbf{H}(\text{div},\Omega) = \{\mathbf{v} \in \mathbf{L}^2(\Omega) : \text{ div } \mathbf{v} \in L^2(\Omega)\}$, $\mathbf{H}_0(\text{div},\Omega) = \{\mathbf{v} \in \mathbf{L}^2(\Omega) : \text{ div } \mathbf{v} \in L^2(\Omega), \mathbf{v}\cdot\boldsymbol{n}_D = 0 \text{ on } \Gamma_D\}$ and $L^2_0(\Omega) = \{q \in L^2(\Omega) : \int_\Omega q = 0\}$.

We define the spaces

$$\mathbf{V} = \{\mathbf{v} \in \mathbf{H}(\text{div},\Omega) : \mathbf{v}_S \in \mathbf{H}^1(\Omega_S), \mathbf{v} = \mathbf{0} \text{ on } \Gamma_S, \text{ and } \mathbf{v}\cdot\boldsymbol{n}_D = 0 \text{ on } \Gamma_D\}$$

and

$$Q = L^2_0(\Omega),$$

with the norms $\|\mathbf{v}\|_{\mathbf{V}} = (|\ \mathbf{v}\ |^2_{1,\Omega_S} + \|\mathbf{v}\|^2_{0,\Omega_D} + \|\ \text{div}\ \mathbf{v}\|^2_{0,\Omega_D})^{\frac{1}{2}} = (|\ \mathbf{v}\ |^2_{1,\Omega_S} + \|\mathbf{v}\|^2_{\mathbf{H}(\text{div},\Omega_D)})^{\frac{1}{2}}$ and $\|q\|_Q = \|q\|_0$ respectively.

The mixed variational formulation of the coupled problem (2.1)-(2.3) can be stated as follow [4, 5, 28, 30]: Find $(\mathbf{u}, p) \in \mathbf{V} \times Q$ that satisfies

$$\begin{cases} a(\mathbf{u},\mathbf{v}) + b(\mathbf{v},p) = F(\mathbf{v}) \quad \forall\, \mathbf{v} \in \mathbf{V}, \\ b(\mathbf{u},q) = G(q) \quad \forall\, q \in Q, \end{cases} \tag{2.4}$$

where the bilinear forms $a(\cdot,\cdot)$ and $b(\cdot,\cdot)$ are defined on $\mathbf{V}\times\mathbf{V}$ and $\mathbf{V}\times Q$, respectively, as:

$$a(\mathbf{u},\mathbf{v}) = \mu\int_{\Omega_S}\nabla\mathbf{u}:\nabla\mathbf{v} + \mu\frac{\alpha}{\sqrt{K}}\int_{\Gamma_I}(\mathbf{u}_S\cdot\boldsymbol{t})\,(\mathbf{v}_S\cdot\boldsymbol{t}) + \frac{\mu}{K}\int_{\Omega_D}\mathbf{u}\cdot\mathbf{v},$$

and

$$b(\mathbf{v},q) = -\int_{\Omega}\operatorname{div}\,\mathbf{v}\,q.$$

By last, the linear forms F and G are defined as:

$$F(\mathbf{v}) = \int_{\Omega_D}\mathbf{f}_D\cdot\mathbf{v} + \int_{\Omega_S}\mathbf{f}_S\cdot\mathbf{v} \quad \text{and} \quad G(q) = -\int_{\Omega_D} g_D\,q.$$

From the classical theory of mixed methods (see, e.g., Theorem and Corollary 4.1 in Chapter I of [25]) it follows the well-posedness of the continuous formulation (2.4) and so the following theorem holds.

Theorem 2.1. *There exists a unique $(\mathbf{u},p)\in\mathbf{V}\times Q$ solution to (2.4). In addition, there exists C, depending on the continuous inf-sup condition constant for b, the coercivity constant (on the null space of b) for a and the boundedness constants for a and b, such that*

$$\|\mathbf{u}\|_{\mathbf{V}} + \|p\|_Q \le C\{\|\mathbf{f}_S\|_{0,\Omega_S} + \|\mathbf{f}_D\|_{0,\Omega_D} + \|g_D\|_{0,\Omega_D}\}.$$

It is well known that the discretization of the velocity and the pressure, for both Stokes and Darcy problems, and the coupled problem, has to be in a particular way to avoid instabilities [1, 2, 3, 6, 7, 8, 10, 11, 12, 14, 19, 24]. In addition, the stable finite element approximations to the Stokes problem could not be appropriate for Darcy problem and, therefore, to the coupled problem under consideration.

In order to develop a unified discretization for the coupled problem, that is, the Stokes and Darcy parts be discretized using the same continuous finite element space, we consider the modification of the Darcy equation introduced in [4, 5]. Indeed, taking the second equation of Darcy' problem (2.2) we can write, for any $\mathbf{v}\in\mathbf{V}$,

$$\int_{\Omega_D}(\operatorname{div}\,\mathbf{u}_D - g_D)\operatorname{div}\,\mathbf{v} = 0. \tag{2.5}$$

Then, by adding this equation to the variational form (see, [4] for details), we get the following modified Stokes-Darcy problem: Find $(\mathbf{u},p)\in\mathbf{V}\times Q$ satisfying

$$\begin{cases} \tilde{a}(\mathbf{u},\mathbf{v}) + b(\mathbf{v},p) = L(\mathbf{v}) & \forall\,\mathbf{v}\in\mathbf{V},\\ b(\mathbf{u},q) = G(q) & \forall\,q\in Q, \end{cases} \tag{2.6}$$

where the bilinear forms $\tilde{a}(\cdot,\cdot)$ and $b(\cdot,\cdot)$ are defined on $\mathbf{V}\times\mathbf{V}$, $\mathbf{V}\times Q$, respectively, as:

$$\tilde{a}(\mathbf{u},\mathbf{v}) = \mu\int_{\Omega_S}\nabla\mathbf{u}:\nabla\mathbf{v} + \frac{\mu}{K}\int_{\Omega_D}\mathbf{u}\cdot\mathbf{v} + \int_{\Omega_D}\operatorname{div}\,\mathbf{u}\operatorname{div}\,\mathbf{v} + \mu\frac{\alpha}{\sqrt{K}}\int_{\Gamma_I}(\mathbf{u}_S\cdot\boldsymbol{t})\,(\mathbf{v}_S\cdot\boldsymbol{t}),$$

and

$$b(\mathbf{v},q) = -\int_{\Omega}\operatorname{div}\,\mathbf{v}\,q.$$

By last, the linear forms L and G are defined as:

$$L(\mathbf{v}) = \int_{\Omega_D} \mathbf{f}_D \cdot \mathbf{v} + \int_{\Omega_S} \mathbf{f}_S \cdot \mathbf{v} + \int_{\Omega_D} g_D \text{ div } \mathbf{v} \quad \text{and} \quad G(q) = -\int_{\Omega_D} g_D\, q.$$

From the classical theory of mixed methods it follows the well-posedness of the continuous formulation (2.6).

Theorem 2.2. *There exists a unique $(\mathbf{u}, p) \in \mathbf{V} \times Q$ solution to (2.6). In addition, there exists a positive constant $\tilde{C}$, depending on the continuous inf-sup condition constant for b, the coercivity constant for $\tilde{a}$ and the boundedness constants for $\tilde{a}$ and b, such that*

$$\|\mathbf{u}\|_{\mathbf{V}} + \|p\|_Q \leq \tilde{C}\{\|\mathbf{f}_S\|_{0,\Omega_S} + \|\mathbf{f}_D\|_{0,\Omega_D} + \|g_D\|_{0,\Omega_D}\}.$$

3. Finite element approximation of the modified Stokes-Darcy problem

In this section, we use the well known $\mathbf{P}_2P_1$ Taylor-Hood elements (see, for example, [13, 16, 17, 21, 26]) in order to approach the velocity and the pressure in the whole domain. Taking into account the modification that we introduced in the section above, this element can be successfully applied to the modified coupled Stokes-Darcy problem.

Let $\{\mathcal{T}_h\}_{h>0}$ be a family of triangulations of Ω such that any two triangles in $\mathcal{T}_h$ share at most a vertex or an edge and each element $T \in \mathcal{T}_h$ is in either Ω_S or Ω_D. Let $\mathcal{T}_h^S$ and $\mathcal{T}_h^D$ be the corresponding induced triangulations of Ω_S and Ω_D. For any $T \in \mathcal{T}_h$, we denote by h_T the diameter of T and ρ_T the diameter of the largest ball inscribed into T and $\eta_T = \frac{h_T}{\rho_T}$. We assume that the family of triangulations is regular, i.e., there exists $\eta > 0$ such that $\eta_T \leq \eta$ for all $T \in \mathcal{T}_h$ and $h > 0$.

Hypothesis **(H1)**: We assume that the triangulation $\mathcal{T}_h$ satisfies that: for $T \in \mathcal{T}_h$, we have that T and Γ_j share at most a vertex or an edge (in particular, T can not have two edges in Γ_j) for $j = S, D, I$.

Let $\mathbf{V}_h \subset \mathbf{V}$ and $Q_h \subset Q$ be finite element spaces. The weak formulation (2.6) leads to the following discrete problem: Find $(\mathbf{v}_h, p_h) \in \mathbf{V}_h \times Q_h$ that satisfies

$$\begin{cases} \tilde{a}(\mathbf{u}_h, \mathbf{v}_h) + b(\mathbf{v}_h, p_h) = L(\mathbf{v}_h) & \forall\, \mathbf{v}_h \in \mathbf{V}_h, \\ b(\mathbf{u}_h, q_h) = G(q_h) & \forall\, q_h \in Q_h. \end{cases} \tag{3.7}$$

The discretization is said to be uniformly stable if there exist constants $\delta, \gamma > 0$, independent of h, such that

$$\begin{aligned} \tilde{a}(\mathbf{v}_h, \mathbf{v}_h) &\geq \delta \|\mathbf{v}_h\|_{\mathbf{V}}^2 \quad \forall\, \mathbf{v}_h \in \mathbf{V}_h, \\ \sup_{\mathbf{0} \neq \mathbf{v}_h \in \mathbf{V}_h} \frac{b(\mathbf{v}_h, q_h)}{||\mathbf{v}_h||_{\mathbf{V}}} &\geq \gamma ||q_h||_Q \quad \forall\, q_h \in Q_h. \end{aligned} \tag{3.8}$$

From now on, we will denote by C a generic positive constant, not necessarily the same at each occurrence, which may depend on the mesh only through the parameter η.

For any subdomain $\mathcal{D} \subseteq \Omega$, $k \in \mathbb{N}$, we denote by $\mathbf{V}_h^k(D)$ be the space of continuous piecewise polynomial vectors of total degree $\leq k$ on T, with $T \in \mathcal{T}_h \cap D$, and let $Q_h^r(D) = \{q \in C^0(\mathcal{D}) : q\,|_T \in \mathcal{P}_r(T)\ \forall\, T \in \mathcal{T}_h \cap \mathcal{D}\}$.

We introduce the following notation

$$\mathcal{E} = \{\text{all edges in } \mathcal{T}_h\}, \quad \mathcal{N} = \{\text{all vertices in } \mathcal{T}_h\},$$

$$\mathcal{M} = \{ \text{ all midpoints of the edges in } \mathcal{T}_h\}.$$

and we denote by N the number of vertices on $\mathcal{N}$ and by M the number of midpoints on $\mathcal{M}$.

Let A be a set, we define

$$\mathcal{E}_A = \{\ell \in \mathcal{E} : \ell \subset A\}, \quad \mathcal{N}_A = \{n \in \mathcal{N} : n \in A\}, \quad \mathcal{M}_A = \{m \in \mathcal{M} : m \in A\}.$$

We decompose

$$\mathcal{E} = \mathcal{E}_{\Omega_S} \cup \mathcal{E}_{\Omega_D} \cup \mathcal{E}_{\Gamma_S} \cup \mathcal{E}_{\Gamma_D} \cup \mathcal{E}_{\Gamma_I}.$$

For $n \in \mathcal{N}$ and $\ell \in \mathcal{E}$ we denote

$$\omega_n = \bigcup\{T \mid T \in \mathcal{T}_h \text{ and } n \in T\} \qquad \omega_\ell := \bigcup_{\mathcal{N}_\ell \cap \mathcal{N}_{T'} \neq \emptyset} T'.$$

We observe that, if M_{ω_ℓ} denotes the numbers of triangles in ω_ℓ then $M_{\omega_\ell} = 2$ if ℓ is an interior edge or $\ell \subset \Gamma_I$ and $M_{\omega_\ell} = 1$ if ℓ is a boundary edge.

For any $T \in \mathcal{T}_h$ we define

$$\omega_T = \bigcup\{\omega_n \mid n \text{ is a vertex of T }\}.$$

For $\ell \in \mathcal{E}_{\Gamma_I}$, we denote by T_S and T_D the two triangles sharing ℓ, with $T_S \in \mathcal{T}_h^S$ and $T_D \in \mathcal{T}_h^D$, and by $\omega_\ell = T_S \cup T_D$. We enumerate the vertices of T_S and T_D so that the vertices of ℓ are numbered first, i.e., let e_1 and e_2 be the vertices of ℓ we denote by e_3^S and e_3^D the vertices in Ω_S and Ω_D respectively. Now, we consider the bubble space introduced in [4]

$$\begin{aligned} B_{3,\ell} := \{v_h \in C^0(\Omega) : v_h \mid_{\omega_\ell} = \mathrm{b}_\ell \psi_{\omega_\ell}, \, \forall\, \ell \in \mathcal{E}_\Gamma, \text{ with } \psi_{\omega_\ell} \in C^0(\omega_\ell), \, \psi_{\omega_\ell} \mid_{T_i} \in P_1(T_i) \\ \text{and } \psi_{\omega_\ell}(e_3^i) = 0, \, i = S \text{ or } D\}. \end{aligned}$$

where b_ℓ denotes the classical edge-bubble function:

$$\mathrm{b}_\ell = \begin{cases} \delta_{e_1,T_i}\delta_{e_2,T_i} & \text{in } T_i,\ i = S \text{ or } D, \\ 0 & \text{in } \Omega \setminus \omega_\ell, \end{cases}$$

The finite element space for the velocities is given by

$$\begin{aligned} \mathbf{V}_h := \{\mathbf{v}_h \in (C^0(\Omega_S))^2, \mathbf{v}_h \in (C^0(\Omega_D))^2 : \mathbf{v}_h \mid_T \in (P_2(T))^2 \quad \forall\, T \in \mathcal{T}_h : \mathcal{E}_T \cap \mathcal{E}_{\Gamma_I} = \emptyset, \\ \text{and } \mathbf{v}_h \mid_T \in (P_2(T))^2 \oplus B_{3,\ell} \mid_T \boldsymbol{n}_\ell \quad \forall\, T \in \mathcal{T}_h : \mathcal{E}_T \cap \mathcal{E}_{\Gamma_I} = \ell, \\ \mathbf{v}_h = 0 \text{ on } \Gamma_S, \mathbf{v}_h \cdot \boldsymbol{n}_D = 0 \text{ on } \Gamma_D \text{ and } \mathbf{v}_h^D \cdot \boldsymbol{n}_D + \mathbf{v}_h^S \cdot \boldsymbol{n}_S = 0 \text{ on } \Gamma_I\} \end{aligned}$$

where $\boldsymbol{n}_\ell$ stands for the unit normal vector on ℓ oriented outward Ω_D.

On the other hand, the finite element space for the pressures is

$$Q_h := \{q_h \in C^0(\Omega_S), q_h \in C^0(\Omega_D) : q_h \mid_T \in P_1(T) \ \forall\ T \in \mathcal{T}_h\} \cap L_0^2(\Omega).$$

Examples of bases for the space $B_{3,\ell}$ have been obtained in [4], we include the description of them here for the sake of completeness. Let $\hat{T}$ be the classical reference triangle, i.e. the triangle of vertices $(0,0), (1,0)$ and $(0,1)$. For each triangle $T \subset \omega_\ell$, we denote by e_1, e_2 and e_3 the vertices of T, such that e_1 and e_2 are the vertices of ℓ and e_3 is the vertex of T that is not on Γ. If we denote by (x_j, y_j), $1 \leq j \leq 3$, the coordinates of the vertices e_j of T, then the affine transformation from $\hat{T}$ onto the triangle of vertices e_1, e_2 and e_3 can be defined as:

$$F(\hat{x}, \hat{y}) = \left(x_3 + (x_1 - x_3)\hat{x} + (x_2 - x_3)\hat{y}, y_3 + (y_1 - y_3)\hat{x} + (y_2 - y_3)\hat{y}\right),$$

which maps the edge $\overline{(1,0)(0,1)}$ into ℓ. In $\hat{T}$ we consider the Lagrange bases $\hat{\beta}_1$ and $\hat{\beta}_2$ such that: $\hat{\beta}_1(\frac{1}{4},\frac{3}{4})=1$, $\hat{\beta}_1(\frac{3}{4},\frac{1}{4})=0$ and $\hat{\beta}_1(0,0)=0$, and $\hat{\beta}_2(\frac{1}{4},\frac{3}{4})=0$, $\hat{\beta}_2(\frac{3}{4},\frac{1}{4})=1$ and $\hat{\beta}_2(0,0)=0$. Therefore, the corresponding bases functions in T are $\beta^{\ell}_{T,i}=\hat{\beta}_i\circ F^{-1}, \quad i=1,2.$

Then, the cubic bubbles $v_{\ell,1}$ and $v_{\ell,2}$ such that, $v_{\ell,i}\mid_T=\delta_{e_1,T}\delta_{e_2,T}\beta^{\ell}_{T,i}$, $i=1,2$ where $\delta_{e_1,T},\delta_{e_2,T}$ and $\delta_{e_3,T}$ denote the barycentric coordinates of $T\in\mathcal{T}_h$. (see Figure 2).

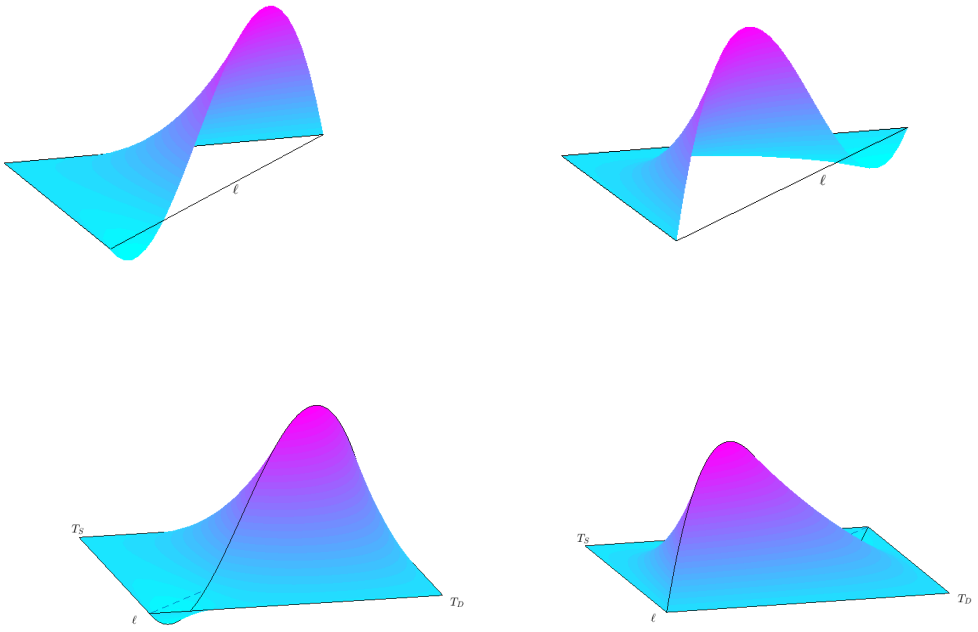

FIGURE 2. The bubble functions $v_{\ell,1}\mid_T$ and $v_{\ell,2}\mid_T$ (top) and $v_{\ell,1}$ and $v_{\ell,2}$ on ω_ℓ (bottom)

We denote by $\{\beta_i\}_{i\in\{1,\cdots,N\}}$, the classical quadratic Lagrange basis of $\mathcal{T}_h$ such that $\beta_i(n_i)=1$ and it is zero at the rest of the nodes of the mesh $\mathcal{T}_h$ and in all the midpoints of $\mathcal{T}_h$; and we denote by $\{\phi_j\}_{j\in\{1,\cdots,M\}}$ be the quadratic bubble Lagrange basis of $\mathcal{T}_h$ such that $\phi_j(m_j)=1$, $m_j\in\mathcal{M}$, and it is zero at the rest of the midpoints of the mesh $\mathcal{T}_h$ and in all vertices of $\mathcal{T}_h$.

The velocity space $\mathbf{V}_h$ consists of all functions $\mathbf{v}=(v_1,v_2)$ of the form

$$\mathbf{v}(x,y)=\sum_{n_i\in\mathcal{N}}\mathbf{v}(n_i)\beta_i(x,y)+\sum_{m_j\in\mathcal{M}}\gamma_j\phi_j(x,y)+\sum_{\ell\in\mathcal{E}_{\Gamma_I}}(\alpha_{\ell,1}v_{\ell,1}(x,y)+\alpha_{\ell,2}v_{\ell,2}(x,y))\boldsymbol{n}_\ell,$$

where $\gamma_j=(\gamma_{j,1},\gamma_{j,2})$ and $\alpha_{\ell,1},\alpha_{\ell,2}$ are constants.

The corresponding pressure space Q_h consists of continuous piecewise linear functions on Ω_D and Ω_S, i.e, functions q of the form

$$q(x,y) = \sum_{n_i \in \mathcal{N}} q(n_i)\lambda_i(x,y),$$

where $\lambda_i \in Q_h^1$, $1 \leq i \leq N$, i.e., $\{\lambda_i\}_{1\leq i\leq N}$ denote the classical Lagrange basis $\lambda_i \mid_T \in P_1(T)$ and $\lambda_i(n_j) = \delta_{ij}$, $1 \leq i,j \leq N$.

We emphasize that all functions in $\mathbf{V}_h$ and Q_h are allowed to be discontinuous across Γ_I.

In order to prove the discrete inf-sup (3.8), we seek for an operator $\mathbf{\Pi}_h : \mathbf{H}_0^1 \longrightarrow \mathbf{V}_h$, such that

$$(P1) \quad b(\mathbf{v} - \mathbf{\Pi}_h\mathbf{v}, q_h) = 0 \quad \forall\, \mathbf{v} \in \mathbf{H}_0^1 \quad \forall\, q_h \in Q_h$$
$$(P2) \quad ||\mathbf{\Pi}_h\mathbf{v}||_{\mathbf{V}} \leq C||\mathbf{v}||_1 \quad \forall\, \mathbf{v} \in \mathbf{H}_0^1$$

where $\|\mathbf{v}\|_1 = (\|v_1\|_1^2 + \|v_2\|_1^2)^{\frac{1}{2}}$.

To define the operator $\mathbf{\Pi}_h$ we follow the ideas given in [4] and [32].

For any $n \in \mathcal{N}$ and $v \in L^2(\omega_n)$, we can define $\mathcal{P}_{\omega_n} : L^2(\omega_n) \to P_0(\omega_n)$ the orthogonal projection of v on $P_0(\omega_n)$ with respect to the internal product in $L^2(\omega_n)$ that fulfills

$$\int_{\omega_n} v\, p_0 = \int_{\omega_n} \mathcal{P}_{\omega_n}(v)\, p_0 \qquad \forall\, p_0 \in P_0(\omega_n),$$

and therefore

$$\mathcal{P}_{\omega_n}(v) = \frac{1}{\mid \omega_n \mid} \int_{\omega_n} v.$$

For any $\mathbf{v} = (v_1, v_2) \in \mathbf{L}^2(\Omega)$ and $n \in \mathcal{N}$ we can define $\mathbf{P}_{\omega_n}(\mathbf{v}) = (\mathcal{P}_{\omega_n}(v_1), \mathcal{P}_{\omega_n}(v_2))$.

We modify the projector in order to consider the different conditions imposed over the vertices when we define the operator

$$\tilde{\mathcal{P}}_{\omega_{n_i}}(v_j) = \begin{cases} \mathcal{P}_{\omega_{n_i}}(v_j) & \text{if } n_i \in \Omega_S,\ n_i \in \Omega_D \text{ or } n_i \in \Gamma^\circ, \\ 0 & \text{if } n_i \in \overline{\Gamma}_S \text{ or } n_i \in \Gamma_D. \end{cases}$$

For any $\mathbf{v} = (v_1, v_2) \in \mathbf{L}^2(\Omega)$ let us consider the following Clément's interpolator in $\mathbf{V}_h^1$ as:

$$\mathcal{I}_1\mathbf{v}(x,y) = \sum_{i=1}^{N} \lambda_i(x,y)\tilde{\mathbf{P}}_{\omega_{n_i}}(\mathbf{v}).$$

We observe that $\mathcal{I}_1\mathbf{v} = \mathbf{0}$ on Γ_D and Γ_S.

For the Clément's interpolator $\mathcal{I}_1\mathbf{v}$ we have the following approximation properties (see, [4, 15, 33]), for any $\mathbf{v} \in \mathbf{H}^1(\Omega)$, $T \in \mathcal{T}_h$,

$$\begin{aligned} \|\mathbf{v} - \mathcal{I}_1\mathbf{v}\|_{m,T} &\leq C h_T^{1-m} \|\mathbf{v}\|_{1,\omega_T} \quad m = 0, 1, \\ \|\mathbf{v} - \mathcal{I}_1\mathbf{v}(x)\|_{0,\ell} &\leq C \mid \ell \mid^{\frac{1}{2}} \|\mathbf{v}\|_{1,\omega_T}, \\ \|\mathbf{v}\|_{1,T} &\leq C\|\mathbf{v}\|_{1,\omega_T}. \end{aligned} \tag{3.9}$$

For any, $n \in \mathcal{N}$, we define $\mathbf{\Pi}_h\mathbf{v}(n) = \mathcal{I}_1\mathbf{v}(n) = \tilde{\mathbf{P}}_{\omega_{n_i}}(\mathbf{v})$, i.e.,

$$\mathbf{\Pi}_h\mathbf{v}(n) = \begin{cases} \mathcal{I}_1\mathbf{v}(n) = \mathbf{P}_{\omega_n}(\mathbf{v}) & \text{if } n \in \Omega_S, n \in \Omega_D \text{ or } n \in \Gamma^\circ, \\ \mathbf{0} & \text{other case,} \end{cases}$$

where Γ° denotes, as usual, the interior of Γ.

We consider $\mathbf{\Pi}_h\mathbf{v} = (\mathbf{\Pi}_{h,1}\mathbf{v}, \mathbf{\Pi}_{h,2}\mathbf{v}) \in \mathbf{V}_h$ of the particular form

$$\begin{aligned}\mathbf{\Pi}_h\mathbf{v} &= \mathcal{I}_1\mathbf{v} + \sum_{j=1}^{M}\gamma_j\phi_j(x,y) + \sum_{\ell\in\mathcal{E}_{\Gamma_I}}(\alpha_{\ell,1}w_{\ell,1}(x,y) + \alpha_{\ell,2}w_{\ell,2}(x,y))\boldsymbol{n}_\ell \\ &= \mathcal{I}_1\mathbf{v} + \mathbf{R}_h\mathbf{v} + \sum_{\ell\in\mathcal{E}_{\Gamma_I}}(\alpha_{\ell,1}w_{\ell,1}(x,y) + \alpha_{\ell,2}w_{\ell,2}(x,y))\boldsymbol{n}_\ell \\ &= \mathcal{I}_1\mathbf{v} + \mathbf{R}_h\mathbf{v} + \mathbf{S}_h\mathbf{v}.\end{aligned} \tag{3.10}$$

First of all, we take $\gamma_j = (\gamma_{j,1}, \gamma_{j,2}) = (0,0)$ for all j such that $m_j \in \mathcal{M}_{\Gamma_k}$, $k = S, D, I$.

We observe that, for each $\ell \in \mathcal{E}_{\Gamma_I}$, we have two degrees of freedom more on ℓ and therefore we can choose $v_\ell = b_\ell\psi_{\omega_\ell}$ such that

$$\int_\ell \mathbf{\Pi}_h\mathbf{v}\cdot\boldsymbol{n}_\ell\,\sigma = \int_\ell \mathbf{v}^D\cdot\boldsymbol{n}_\ell\,\sigma, \quad \forall\,\sigma\in P_1(\ell), \tag{3.11}$$

or equivalently (in view of $\gamma_j = \mathbf{0}$, when $m_j \in \Gamma_I$),

$$\int_\ell b_\ell\psi_{\omega_\ell}\,\sigma = \int_\ell(\mathbf{v}^D - \mathcal{I}_1\mathbf{v})\cdot\boldsymbol{n}_\ell\,\sigma, \quad \forall\,\sigma\in P_1(\ell).$$

We note that this relation impose exactly two conditions on ψ_{ω_ℓ}, and since we have two degrees of freedom of ψ_{ω_ℓ} the existence (and so the uniqueness) of ψ_{ω_ℓ} is guarantee (see [4] for details). Indeed, since for each $T \subset \omega_\ell$, the function $\psi_{\omega_\ell}\mid_T$ can be written as $\psi_{\omega_\ell}\mid_T = \alpha_{\ell,1}\beta^\ell_{T,1} + \alpha_{\ell,2}\beta^\ell_{T,2}$, the parameters $\alpha_{\ell,1}$ and $\alpha_{\ell,2}$ can be easily obtained by solving the non singular system (3.11). Moreover, if we denote by $\beta_{\omega_\ell,j}$ the linear continuous functions defined in ω_ℓ such that $\beta_{\omega_\ell,j}\mid_T = \beta^\ell_{T,j}$, $j = 1,2$, we can compute $\alpha_{\ell,1}$ and $\alpha_{\ell,2}$ and an easy calculation shows that

$$\mid\alpha_{\ell,j}\mid \leq \frac{C}{\mid\ell\mid}\max_{j=1,2}\mid\int_\ell(\mathbf{v}^D - \mathcal{I}_1\mathbf{v}(n))\cdot\boldsymbol{n}_\ell\;\beta_{\omega_\ell,j}\mid. \tag{3.12}$$

Therefore, the operator $\mathbf{S}_h\mathbf{v}$ is uniquely determined.

Now, we define γ_ℓ for each $\ell \in \mathcal{E}_{\Omega_S}\cup\mathcal{E}_{\Omega_D}$ as follows

$$\gamma_\ell = (\gamma_{\ell,1},\gamma_{\ell,2}) = \left(\frac{\mid\omega_\ell\mid}{3}\right)^{-1}\left(\sum_{T\in\omega_\ell}\int_T \mathbf{t}'_{\ell,T}\cdot(\mathbf{v} - \mathcal{I}_1\mathbf{v} - \mathbf{S}_h\mathbf{v})\right)\mathbf{t}_\ell \tag{3.13}$$

where $\mathbf{t}_\ell$ is a unit tangent vector to ℓ and the dual vectors $\mathbf{t}'_{\ell,T}$ are chosen as follows.

For each $T \in \mathcal{T}_h$, the edge ℓ is numbered first by ℓ_1 and the others edges of T by ℓ_2 and ℓ_3. Let $\mathbf{t}_{1,T}, \mathbf{t}_{2,T}$ and $\mathbf{t}_{3,T}$ be the tangential vectors to the edges ℓ_1, ℓ_2 and ℓ_3 respectively.

Then, if $T \in \omega_\ell$, with $\ell \in \mathcal{E}_{\Omega_S}\cup\mathcal{E}_{\Omega_D}$, the dual vectors $\mathbf{t}'_{1,T}$, $\mathbf{t}'_{2,T}$ and $\mathbf{t}'_{3,T}$ are defined as:

$$\mathbf{t}'_{k,T} = \sum_{i=1}^{2}A_{k,i}\mathbf{t}_{i,T}, \quad k = 1,2 \qquad \mathbf{t}'_{3,T} = 0$$

with

$$A = \frac{1}{1-(\mathbf{t}_{1,T}\cdot\mathbf{t}_{2,T})^2}\begin{pmatrix} 1 & -\mathbf{t}_{1,T}\cdot\mathbf{t}_{2,T} \\ -\mathbf{t}_{1,T}\cdot\mathbf{t}_{2,T} & 1 \end{pmatrix} = \frac{1}{\sin^2(\theta_T)}\begin{pmatrix} 1 & -\cos(\theta_T) \\ -\cos(\theta_T) & 1 \end{pmatrix}$$

with $\mathbf{t}_{1,T}\cdot\mathbf{t}_{2,T} = \cos(\theta_T)$, $0 < \theta_T < \pi$.

In view of Lemma 2.1 of [32], we have that for any $\mathbf{z}\in\mathbb{R}^2$, $T\in\mathcal{T}_h$, we can write

$$\mathbf{z} = \sum_{j=1}^{2}(\mathbf{t}_{j,T}\cdot\mathbf{z})\mathbf{t}'_{j,T} = \sum_{j=1}^{3}(\mathbf{t}_{j,T}\cdot\mathbf{z})\mathbf{t}'_{j,T}. \tag{3.14}$$

Thus,

$$\gamma_\ell = \begin{cases} \left(\frac{|\,\omega_\ell\,|}{3}\right)^{-1}\left(\sum_{T\in\omega_\ell}\int_T \mathbf{t}'_{\ell,T}\cdot(\mathbf{v}-\mathcal{I}_1\mathbf{v}-\mathbf{S}_h\mathbf{v})\right)\mathbf{t}_\ell & \text{if } \ell\in\mathcal{E}_{\Omega_S} \text{ or } \ell\in\mathcal{E}_{\Omega_D}, \\ \mathbf{0} & \text{if } \ell\in\mathcal{E}_{\Gamma_k} \text{ for } k=S,D,I. \end{cases} \tag{3.15}$$

Now, we are in conditions of verify the $(P1)$ property of the operator $\mathbf{\Pi}_h\mathbf{v}$.

Lemma 3.1. *Let be $\mathbf{v}\in\mathbf{H}^1_0$. The operator $\mathbf{\Pi}_h\mathbf{v}$ is such that*

$$b(\mathbf{v}-\mathbf{\Pi}_h\mathbf{v}, q_h) = 0 \qquad \forall\, q_h\in Q_h.$$

Proof of Lemma 3.1. Since $b(\mathbf{v}-\mathbf{\Pi}_h\mathbf{v},q_h) = -\int_{\Omega_D}\text{ div }(\mathbf{v}-\mathbf{\Pi}_h\mathbf{v})\,q_h - \int_{\Omega_S}\text{ div }(\mathbf{v}-\mathbf{\Pi}_h\mathbf{v})\,q_h$, adding on all triangles in both domains, integrating by parts on each triangle we get

$$\begin{aligned} b(\mathbf{v}-\mathbf{\Pi}_h\mathbf{v},q_h) &= -\sum_{T\subset\Omega_D}\int_T \text{div }(\mathbf{v}-\mathbf{\Pi}_h\mathbf{v})\,q_h - \sum_{T\subset\Omega_S}\int_T \text{div }(\mathbf{v}-\mathbf{\Pi}_h\mathbf{v})\,q_h \\ &= \sum_{T\subset\Omega_D}\left(\int_T(\mathbf{v}-\mathbf{\Pi}_h\mathbf{v})\cdot\nabla q_h - \int_{\partial T} q_h(\mathbf{v}-\mathbf{\Pi}_h\mathbf{v})\cdot\boldsymbol{n}_D\right) + \\ &\quad \sum_{T\subset\Omega_S}\left(\int_T(\mathbf{v}-\mathbf{\Pi}_h\mathbf{v})\cdot\nabla q_h - \int_{\partial T} q_h(\mathbf{v}-\mathbf{\Pi}_h\mathbf{v})\cdot\boldsymbol{n}_S\right). \end{aligned}$$

For any $\ell\in\mathcal{E}_{\Omega_S}\cup\mathcal{E}_{\Omega_D}$ we choose a unit normal vector $\mathbf{n}_\ell$ and denote the two triangles sharing this edge T_{in} and T_{out}, with $\boldsymbol{n}_\ell$ pointing outwards T_{out}. We define

$$[\![\mathbf{v}\cdot\boldsymbol{n}_\ell]\!]_\ell := \left(\mathbf{v}\,|_{T_{\text{out}}}\right)\cdot\boldsymbol{n}_\ell - \left(\mathbf{v}\,|_{T_{\text{in}}}\right)\cdot\boldsymbol{n}_\ell,$$

which corresponds to the jump of the normal component of $\mathbf{v}$ across the edge ℓ. Notice that this value is independent of the chosen direction of the normal vector $\boldsymbol{n}_\ell$.

Rewriting the integrals on the borders of the triangles, we obtain

$$\begin{aligned} b(\mathbf{v}-\mathbf{\Pi}_h\mathbf{v},q_h) &= \sum_{T\subset\Omega_D}\int_T(\mathbf{v}-\mathbf{\Pi}_h\mathbf{v})\cdot\nabla q_h+\sum_{T\subset\Omega_S}\int_T(\mathbf{v}-\mathbf{\Pi}_h\mathbf{v})\cdot\nabla q_h \\ &- \frac{1}{2}\sum_{T\subset\Omega_D}\sum_{\ell\in\mathcal{E}_T\cap\Omega_D}\int_\ell[\![(\mathbf{v}-\mathbf{\Pi}_h\mathbf{v})\cdot\mathbf{n}_\ell]\!]_\ell\ q_h-\sum_{\ell\in\mathcal{E}_{\Gamma_D}}\int_\ell(\mathbf{v}-\mathbf{\Pi}_h\mathbf{v})\cdot\boldsymbol{n}_D\,q_h \\ &- \sum_{\ell\in\mathcal{E}_\Gamma}[\int_\ell(\mathbf{v}^D-\mathbf{\Pi}_h\mathbf{v})\cdot\ \boldsymbol{n}_D\,q_{D,h}+\int_\ell(\mathbf{v}^S-\mathbf{\Pi}_h\mathbf{v})\cdot\ \boldsymbol{n}_S\,q_{S,h}] \\ &- \frac{1}{2}\sum_{T\subset\Omega_S}\sum_{\ell\in\mathcal{E}_T\cap\Omega_S}\int_\ell[\![(\mathbf{v}-\mathbf{\Pi}_h\mathbf{v})\cdot\mathbf{n}_\ell]\!]_\ell\ q_h-\sum_{\ell\in\mathcal{E}_{\Gamma_S}}\int_\ell(\mathbf{v}-\mathbf{\Pi}_h\mathbf{v})\cdot\boldsymbol{n}_S\,q_h. \end{aligned}$$

Now, since $\mathbf{\Pi}_h\mathbf{v}=\mathbf{0}$ in Γ_S and Γ_D, from the boundary conditions and continuity of the normal component of $\mathbf{v}$ and $\mathbf{\Pi}_h\mathbf{v}$ we have that

$$\begin{aligned} b(\mathbf{v}-\mathbf{\Pi}_h\mathbf{v},q_h) &= \sum_{T\subset\Omega_D}\int_T(\mathbf{v}-\mathbf{\Pi}_h\mathbf{v})\cdot\nabla q_h+\sum_{T\subset\Omega_S}\int_T(\mathbf{v}-\mathbf{\Pi}_h\mathbf{v})\cdot\nabla q_h \\ &- \sum_{\ell\in\mathcal{E}_{\Gamma_I}}[\int_\ell(\mathbf{v}^D-\mathbf{\Pi}_h\mathbf{v})\cdot\ \boldsymbol{n}_D\,q_{D,h}+\int_\ell(\mathbf{v}^S-\mathbf{\Pi}_h\mathbf{v})\cdot\ \boldsymbol{n}_S\,q_{S,h}] \\ &= \int_{\Omega_D}(\mathbf{v}-\mathbf{\Pi}_h\mathbf{v})\cdot\nabla q_h+\int_{\Omega_S}(\mathbf{v}-\mathbf{\Pi}_h\mathbf{v})\cdot\nabla q_h \\ &- \sum_{\ell\in\mathcal{E}_{\Gamma_I}}[\int_\ell(\mathbf{v}^D-\mathbf{\Pi}_h\mathbf{v})\cdot\ \boldsymbol{n}_D\,q_{D,h}+\int_\ell(\mathbf{v}^S-\mathbf{\Pi}_h\mathbf{v})\cdot\ \boldsymbol{n}_S\,q_{S,h}] \\ &= I+II+III. \end{aligned}$$

We analyze the value of each of the previous terms:

I - II) For any $\mathbf{w}\in\mathbf{V}_h^2$ we have that

$$\int_T\mathbf{w}=\frac{|T|}{3}\sum_{m\in T\cap\mathcal{M}}\mathbf{w}(m) \tag{3.16}$$

since the integration rule of the midpoints is exact for quadratic functions. As $q_h\in Q_h^1$, its gradient is constant and since $\mathbf{R}_h\mathbf{v}(m_\ell)=\mathbf{0}$ if $m_\ell\in\Gamma_I,\Gamma_D$ or Γ_S, we have

$$\int_{\Omega_k}\mathbf{R}_h\mathbf{v}\cdot\nabla q_h=\sum_{\ell\in\mathcal{E}_{\Omega_k}}\sum_{j=1}^{2}\frac{|\ T_{\ell,j}\ |}{3}\nabla q_h\ |_{T_{\ell,j}}\cdot\mathbf{R}_h\mathbf{v}(m_\ell)$$

where $T_{\ell,j}$, $j=1,2$, denotes the two triangles on ω_ℓ.
Then, from (3.15) we get

$$\int_{\Omega_k} \mathbf{R}_h\mathbf{v}\cdot\nabla q_h$$
$$= \sum_{\ell\in\mathcal{E}_{\Omega_k}}\sum_{j=1}^{2}\frac{|\,T_{\ell,j}\,|}{3}\nabla q_h\,|_{T_{\ell,j}}\cdot\left(\frac{|\,\omega_\ell\,|}{3}\right)^{-1}\sum_{i=1}^{2}\left(\int_{T_{\ell,i}}\mathbf{t}'_{\ell,T_{\ell,i}}\cdot(\mathbf{v}-\mathcal{I}_1\mathbf{v}-\mathbf{S}_h\mathbf{v})\right)\mathbf{t}_\ell.$$

For any $\ell\in\mathcal{E}_{\Omega_S}\cup\mathcal{E}_{\Omega_D}$, $T,T'\in\omega_\ell$ and $q\in Q_h^1$ we have that $\nabla q_h\,|_T\cdot\mathbf{t}_\ell=\nabla q_h\,|_{T'}\cdot\mathbf{t}_\ell$ which we can simply denote as $(\nabla q_h\cdot\mathbf{t})_\ell$. Thus,

$$\int_{\Omega_k} \mathbf{R}_h\mathbf{v}\cdot\nabla q_h$$
$$= \sum_{\ell\in\mathcal{E}_{\Omega_k}}\sum_{j=1}^{2}\frac{|\,T_{\ell,j}\,|}{3}\nabla q_h\,|_{T_{\ell,j}}\cdot\left(\frac{|\,\omega_\ell\,|}{3}\right)^{-1}\sum_{i=1}^{2}\left(\int_{T_{\ell,i}}\mathbf{t}'_{\ell,T_{\ell,i}}\cdot(\mathbf{v}-\mathcal{I}_1\mathbf{v}-\mathbf{S}_h\mathbf{v})\right)\mathbf{t}_\ell$$
$$= \sum_{\ell\in\mathcal{E}_{\Omega_k}}(\nabla q_h\cdot\mathbf{t})_\ell\sum_{j=1}^{2}\frac{|\,T_{\ell,j}\,|}{3}\left(\frac{|\,\omega_\ell\,|}{3}\right)^{-1}\sum_{i=1}^{2}\left(\int_{T_{\ell,i}}\mathbf{t}'_{\ell,T_{\ell,i}}\cdot(\mathbf{v}-\mathcal{I}_1\mathbf{v}-\mathbf{S}_h\mathbf{v})\right)$$
$$= \sum_{\ell\in\mathcal{E}_{\Omega_k}}(\nabla q_h\cdot\mathbf{t})_\ell\sum_{i=1}^{2}\left(\int_{T_{\ell,i}}\mathbf{t}'_{\ell,T_{\ell,i}}\cdot(\mathbf{v}-\mathcal{I}_1\mathbf{v}-\mathbf{S}_h\mathbf{v})\right).$$

Using again that, for $T_{\ell,1}$ and $T_{\ell,2}$ in ω_ℓ, we have that $(\nabla q_h\cdot\mathbf{t})_\ell=\nabla q_h\,|_{T_{\ell,1}}\cdot\mathbf{t}_{\ell,T_{\ell,1}}=\nabla q_h\,|_{T_{\ell,2}}\cdot\mathbf{t}_{\ell,T_{\ell,2}}$ and grouping the terms we get

$$\int_{\Omega_k}\mathbf{R}_h\mathbf{v}\cdot\nabla q_h=\sum_{T\in\mathcal{T}_h\cap\Omega_k}\int_T\left(\sum_{s=1}^{3}\nabla q_h\,|_T\cdot\mathbf{t}_{s,T}\mathbf{t}'_{s,T}\right)\cdot(\mathbf{v}-\mathcal{I}_1\mathbf{v}-\mathbf{S}_h\mathbf{v}).$$

Now, from (3.14) we conclude that

$$\begin{aligned}\int_{\Omega_k}\mathbf{\Pi}_h\mathbf{v}\cdot\nabla q_h&=\int_{\Omega_k}\mathcal{I}_1\mathbf{v}\cdot\nabla q_h+\sum_{T\in\mathcal{T}_h\cap\Omega_k}\int_T\nabla q_h\,|_T\cdot(\mathbf{v}-\mathcal{I}_1\mathbf{v}-\mathbf{S}_h\mathbf{v})\\&\quad+\int_{\Omega_k}\mathbf{S}_h\mathbf{v}\cdot\nabla q_h\\&=\int_{\Omega_k}\nabla q_h\cdot\mathbf{v}.\end{aligned}$$

III) If $\ell\in\mathcal{E}_{\Gamma_I}$, as $\mathbf{v}\in\mathbf{H}_0^1(\Omega)$ its normal component is continuous and $\mathbf{n}_D=-\mathbf{n}_S$, we have that $\int_\ell(\mathbf{v}^S-\mathbf{\Pi}_h\mathbf{v})\cdot\boldsymbol{n}_S\,q_{S,h}=\int_\ell(\mathbf{\Pi}_h\mathbf{v}-\mathbf{v}^D)\cdot\boldsymbol{n}_D\,q_{S,h}$. Thus, to prove that $\int_\ell(\mathbf{v}^D-\mathbf{\Pi}_h\mathbf{v})\cdot\boldsymbol{n}_D\,q_{D,h}+\int_\ell(\mathbf{v}^S-\mathbf{\Pi}_h\mathbf{v})\cdot\boldsymbol{n}_S\,q_{S,h}=0$ it is enough to see that

$$\int_\ell\mathbf{\Pi}_h\mathbf{v}\cdot\boldsymbol{n}_D\,\sigma=\int_\ell\mathbf{v}^D\cdot\boldsymbol{n}_D\,\sigma\quad\forall\,\sigma\in P_1(\ell),$$

which holds from (3.11).

□

Now, we obtain the $\mathbf{H}^1$ bound of our operator.

Lemma 3.2. *There exists a constant $C > 0$, independent of h, such that*

$$\|\mathbf{\Pi}_h\mathbf{v}\|_{\mathbf{V}} = (\mid \mathbf{\Pi}_h\mathbf{v} \mid^2_{1,\Omega_S} + \|\mathbf{\Pi}_h\mathbf{v}\|^2_{\mathbf{H}(div,\Omega_D)})^{\frac{1}{2}} \leq C\|\mathbf{v}\|_1 \quad \forall\, \mathbf{v} \in \mathbf{H}^1_0.$$

Proof of Lemma 3.2. We observe that, it is enough to prove that there exists a constant C such that

$$\mid \mathbf{\Pi}_h\mathbf{v} \mid^2_{1,\Omega_S} = \mid \mathbf{\Pi}_{h,1}\mathbf{v} \mid^2_{1,\Omega_S} + \mid \mathbf{\Pi}_{h,2}\mathbf{v} \mid^2_{1,\Omega_S} \leq C\|\mathbf{v}\|^2_1,$$

in view of $\|\mathbf{\Pi}_h\mathbf{v}\|_{\mathbf{H}(\mathrm{div},\Omega_D)} \leq \|\mathbf{\Pi}_h\mathbf{v}\|_{1,\Omega_D}$, and the fact that bound for $\mid \mathbf{\Pi}_{h,j}\mathbf{v} \mid_{1,\Omega_D}$ is completely analogous.

We write

$$\mid \mathbf{\Pi}_{h,j}\mathbf{v} \mid^2_{1,\Omega_S} = \sum_{T\subset\Omega_S:\mathcal{E}_T\cap\mathcal{E}_\Gamma=\emptyset} \mid \mathbf{\Pi}_{h,j}\mathbf{v} \mid^2_{1,T} + \sum_{T\subset\Omega_S:\mathcal{E}_T\cap\mathcal{E}_\Gamma\neq\emptyset} \mid \mathbf{\Pi}_{h,j}\mathbf{v} \mid^2_{1,T} = I + II \quad j = 0, 1.$$

First, we analyze the term $I = \sum_{T\subset\Omega_S:\mathcal{E}_T\cap\mathcal{E}_\Gamma=\emptyset} \mid \mathbf{\Pi}_{h,j}\mathbf{v} \mid^2_{1,T}$. Here the operator is

$$\mathbf{\Pi}_{h,j}\mathbf{v} \mid_T = \mathcal{I}_{1,j}\mathbf{v} \mid_T + \mathbf{R}_{h,j}\mathbf{v} \mid_T .$$

If we denote by ϕ_1, ϕ_2 and ϕ_3 the quadratic Lagrange bases of T, such that $\phi_j(m_i) = \delta_{ij}$, $m_i \in \mathcal{M}_T$, $i, j = 1, 2, 3$ and it is zero in all vertices of T then,

$$I \leq C\left(\sum_{T\subset\Omega_S:\mathcal{E}_T\cap\mathcal{E}_\Gamma=\emptyset} \mid \mathcal{I}_{1,j}\mathbf{v} \mid^2_{1,T} + \sum_{T\subset\Omega_S:\mathcal{E}_T\cap\mathcal{E}_\Gamma=\emptyset}\sum_{i=1}^{3} \mid \gamma_{\ell_i,j}\phi_i \mid^2_{1,T}\right)$$

with $m_i \in \ell_i$, $i = 1, 2, 3$.

It's easy to prove that $\mid \mathcal{I}_{1,j}\mathbf{v} \mid_{1,T} \leq C\|\mathbf{v}\|_{1,\omega_T}$, $j = 1, 2$ (see [4] for details). On the other hand, from (3.15) (we recall that in the case under consideration $\mathbf{S}_h\mathbf{v} = \mathbf{0}$) it concludes

$$\mid \gamma_{\ell_i,j} \mid \leq C \mid \omega_{\ell_i} \mid^{-1} \sum_{T\in\omega_{\ell_i}} \|\mathbf{v} - \mathcal{I}_1\mathbf{v}\|_{0,T} \mid T \mid^{\frac{1}{2}} .$$

Now, using $|T|^{\frac{1}{2}} \sim h_T$, the Clément's properties (3.9) and the regularity of the mesh we obtain

$$\mid \gamma_{\ell_i,j} \mid \leq C \mid \omega_{\ell_i} \mid^{-1} \sum_{T\in\omega_{\ell_i}} h_T^2\|\mathbf{v}\|_{1,\omega_T} \leq C \sum_{T\in\omega_{\ell_i}} \|\mathbf{v}\|_{1,\omega_T} \quad i = 1, 2, 3.$$

Therefore, since the regularity of the mesh we have that the number of triangles in a neighborhood ω_T is bounded by a uniform constant we get

$$I \leq C\left(\sum_{T\subset\Omega_S:\mathcal{E}_T\cap\mathcal{E}_\Gamma=\emptyset} \mid \mathcal{I}_{1,j}\mathbf{v} \mid^2_{1,T} + \sum_{T\subset\Omega_S:\mathcal{E}_T\cap\mathcal{E}_\Gamma=\emptyset} \|\mathbf{v}\|_{1,\omega_T}\right) \leq C\|\mathbf{v}\|_{1,\Omega_S}.$$

Now, we analyze the term $II = \sum_{T\in\Omega_S:\mathcal{E}_T\cap\mathcal{E}_\Gamma\neq\emptyset} \mid \mathbf{\Pi}_{h,j}\mathbf{v} \mid^2_{1,T}$, i.e., the case in which T has only one side on the interface that we denoted by ℓ.

$$
\begin{aligned}
II \leq & C \Bigg(\sum_{T\subset\Omega_S:\mathcal{E}_T\cap\mathcal{E}_\Gamma\neq\emptyset} |\, \mathcal{I}_{1,j}\mathbf{v}\,|^2_{1,T} + \sum_{T\subset\Omega_S:\mathcal{E}_T\cap\mathcal{E}_\Gamma\neq\emptyset} |\, \mathbf{R}_{h,j}\mathbf{v}\,|^2_{1,T} \\
& + \sum_{T\subset\Omega_S:\mathcal{E}_T\cap\mathcal{E}_\Gamma\neq\emptyset} |\, \mathbf{S}_{h,j}\mathbf{v}\,|^2_{1,T} \Bigg).
\end{aligned} \tag{3.17}
$$

Hence,

$$
\begin{aligned}
\int_T (v_\ell n_{\ell,j})^2 &= \int_T (\delta_{e_1,T}\,\delta_{e_2,T}\,\psi_{\omega_\ell} n_{\ell,j})^2 \\
&= \int_T \Big((\alpha_{\ell,1}\delta_{e_1,T}\,\delta_{e_2,T}\,\beta^\ell_{T,1} + \alpha_{\ell,2}\delta_{e_1,T}\,\delta_{e_2,T}\,\beta^\ell_{T,2}) n_{\ell,j} \Big)^2 \\
&\leq C \max_{i=1,2} |\, \alpha_{\ell,i}\,|^2 \|\delta_{e_1,T}\,\delta_{e_2,T}\|^2_{0,T} \\
&\leq C \frac{1}{|\,\ell\,|} \|\mathbf{v} - I_1\mathbf{v}(x)\|^2_{0,\ell} \|\delta_{e_1,T}\,\delta_{e_2,T}\|^2_{0,T} \\
&\leq C \frac{|T|}{|\,\ell\,|} \|\mathbf{v} - I_1\mathbf{v}(x)\|^2_{0,\ell} \leq C h_T^2 \|\mathbf{v}\|^2_{1,\omega_T}
\end{aligned}
$$

where we use that $\int_T \delta^{n_1}_{e_1,T}\delta^{n_2}_{e_2,T}dx = \frac{n_1!n_2!2!}{(n_1+n_2+2)!}|T|$ and (3.9).
Now, by using a classical inverse inequality, we get

$$
|\, v_\ell n_{\ell,j}\,|_{1,T} \leq C \frac{1}{h_T} \|v_\ell n_{\ell,j}\|_{0,T} \leq C\|\mathbf{v}\|_{1,\omega_T}
$$

and therefore

$$
|\, \mathbf{S}_{h,j}\mathbf{v}\,|_{1,T} \leq C\|\mathbf{v}\|_{1,\omega_T}. \tag{3.18}
$$

On the other hand, in view of $\gamma_{\ell_i} = \mathbf{0}$ for $m_i \in \Gamma_I$, if we denote by ϕ_1, ϕ_2 and ϕ_3 the Lagrange basis associated to the midpoints of T such that m_1 is the midpoint in $\ell_1 \subset \Gamma_I$, then from (3.10), (3.15) and (3.18) we have

$$
\begin{aligned}
|\, \mathbf{R}_{h,j}\mathbf{v}\,|_{1,T} &\leq |\, \gamma_{\ell_2,j}\phi_2\,|_{1,T} + |\, \gamma_{\ell_3,j}\phi_3\,|_{1,T} \\
&\leq C \sum_{i=2,3} |\, \omega_{\ell_i}\,|^{-1} \sum_{T\subset\omega_{\ell_i}} \left(\|\mathbf{v} - I_1\mathbf{v}\|_{0,T} + \|\mathbf{S}_h\mathbf{v}\|_{0,T} \right) |T|^{\frac{1}{2}} \\
&\leq C \sum_{i=2,3} \sum_{T\subset\omega_{\ell_i}} \|\mathbf{v}\|_{1,\omega_T}.
\end{aligned}
$$

Therefore, by using these estimations in the expression (3.17) of the operator we get

$$
II \leq C \sum_{T\subset\Omega_S:\mathcal{E}_T\cap\mathcal{E}_\Gamma\neq\emptyset} \|\mathbf{v}\|^2_{1,\omega_T} \leq C\|\mathbf{v}\|^2_1.
$$

Finally,

$$
|\, \mathbf{\Pi}_h\mathbf{v}\,|_{1,\Omega_S} \leq C\|\mathbf{v}\|_1
$$

and the proof concludes. □

Remark 3.1. *We observe that, if we define the operator* $\mathbf{I}_h : \mathbf{H}_0^1(\Omega) \to \mathbf{V}_h$ *as*

$$\mathbf{I}_h\mathbf{v} = \sum_{j=1}^{M} \delta_j \phi_j(x,y) + \sum_{\ell \in \mathcal{E}_{\Gamma_I}} (\alpha_{\ell,1} v_{\ell,1}(x,y) + \alpha_{\ell,2} v_{\ell,2}(x,y)) \boldsymbol{n}_\ell,$$

with $\delta_j = \mathbf{0}$ *if* $m_j \in \Gamma_k$, $k = S, D, I$, *and* $\alpha_{\ell,1}$ *and* $\alpha_{\ell,2}$ *such that*

$$\int_\ell \mathbf{I}_h\mathbf{v} \cdot \boldsymbol{n}_D \, \sigma = \int_\ell \mathbf{v}^D \cdot \boldsymbol{n}_D \, \sigma \quad \forall \, \sigma \in P_1(\ell),$$

and

$$\delta_j = \left(\frac{\mid \omega_\ell \mid}{3} \right)^{-1} \left(\sum_{T \in \omega_\ell} \int_T \mathbf{t}'_{\ell,T} \cdot (\mathbf{v} - \tilde{S}_h\mathbf{v}) \right) \mathbf{t}_\ell \qquad \text{if } m_j \in \Omega_S \text{ or } m_j \in \Omega_D$$

where $\tilde{S}_h\mathbf{v} = \sum_{\ell \in \mathcal{E}_{\Gamma_I}} (\alpha_{\ell,1} v_{\ell,1}(x,y) + \alpha_{\ell,2} v_{\ell,2}(x,y)) \boldsymbol{n}_\ell$.

This operator satisfies the property $(P1)$ *and there exists a constant* C *such that* $\|\mathbf{I}_h\mathbf{v}\|_0 \leq C\|\mathbf{v}\|_0$. *However, this operator does not satisfy property* $(P2)$.

Theorem 3.1. *There exists a unique solution* $(\mathbf{u}_h, p_h) \in \mathbf{V}_h \times Q_h$ *to the problem (3.7).*

Proof of Theorem 3.1. From Lemmas 3.1 and 3.2, we have that our interpolator $\mathbf{\Pi}_h\mathbf{v}$ satisfies the conditions (P_1) and (P_2). Therefore this theorem is a direct consequence of the fact that the bilinear form $\tilde{a}$ is coercive and continuous, b is continuous and satisfies the discrete inf-sup condition, together with the abstract theory of mixed problems [13]. □

Hence, from theory of mixed problems, we immediately have the following.

Corollary 3.1. *Let* $(\mathbf{u}, p) \in \mathbf{V} \times Q$ *be the solution of the weak formulation (2.6) of the coupled problem. Let* $(\mathbf{u}_h, p_h) \in \mathbf{V}_h \times Q_h$ *be the solution of the discrete problem (3.7). Let the finite element spaces be chosen as in section 3. Then, there exists a constant* C *such that:*

$$\|\mathbf{u} - \mathbf{u}_h\|_{\mathbf{V}} + \|p - p_h\|_Q \leq C\{ \inf_{\mathbf{v}_h \in \mathbf{V}_h} \|\mathbf{u} - \mathbf{v}_h\|_{\mathbf{V}} + \inf_{q_h \in Q_h} \|p - q_h\|_Q \}.$$

4. Numerical experiments

We end this paper with three numerical experiments which show the good performance of our method. We defined the individual errors by,

$$e_0(p_S) = \|p_S - p_{S,h}\|_{0,\Omega_S} \qquad e_0(p_D) = \|p_D - p_{D,h}\|_{0,\Omega_D}$$
$$e_0(\text{div } \mathbf{v}_S) = \|\text{div}(\mathbf{v}_S - \mathbf{v}_{S,h})\|_{0,\Omega_S} \qquad e_0(\text{div } \mathbf{v}_D) = \|\text{div}(\mathbf{v}_D - \mathbf{v}_{D,h})\|_{0,\Omega_D}$$
$$e_1(\mathbf{v}_S) = \mid \mathbf{v}_S - \mathbf{v}_{S,h} \mid_{1,\Omega_S}$$

and the rates of convergence given by,

$$r_i(\square) = \frac{log(\frac{e_i(\square)}{e'_i(\square)})}{log(\frac{h}{h'})} \qquad \square \in \{\mathbf{v}_S, \text{div } \mathbf{v}_S, \text{div } \mathbf{v}_D, p_S, p_D\} \text{ and } i = 0, 1$$

where h and h' denote two consecutive mesh-sizes with errors e_i and e'_i.

Using the previous definition of r_i, we present in Tables 1 and 2, the convergence history for a set of shape regular triangulations of the domain for the first example, in Tables 3 and 4, the corresponding for the second one and in Tables 5 and 6 the corresponding for the last numerical experiment. For simplicity, all the parameters such as K, α and μ are set to 1. We mention that, since is difficult to construct examples satisfying the entire coupled Stokes-Darcy problem (2.1)-(2.3) (in particular, the homogeneous interface conditions (2.3)), the numerical experiments could include nonhomogeneous terms for the interface conditions and therefore conduce to modify (only) the right-hand side in (2.6).

We also comment that, in practice, mass conservation and Neumann condition have to be impose in a weak way. Indeed, when we assembling the system matrix we must add equations that ensure the normal continuity of the velocity and the boundary condition, i. e., $\int_\Gamma(\mathbf{v}_h^D\cdot\boldsymbol{n}_D+\mathbf{v}_h^S\cdot\boldsymbol{n}_S)\,\gamma=0,\ \forall\,\gamma\in\{C^0(\Gamma):\gamma\mid_\ell\in P_2(\ell)\oplus(B_{3,\ell})\mid_\ell\}$ and $\int_{\Gamma_D}\mathbf{v}_h^D\cdot\boldsymbol{n}_D\,\lambda=0,\ \forall\,\lambda\in\{C^0(\Gamma):\lambda\mid_\ell\in P_2(\ell)\}$.

First example : Let $\Omega_D=(-\frac{1}{2},\frac{1}{2})\times(-\frac{1}{2},\frac{1}{2})$ and $\Omega_S=(-1,1)\times(-1,1)\setminus\Omega_D$ be a porous medium completely surrounded by a fluid (see Figure 3). The particularity of this example is that there is no Γ_D because the boundary of Ω_D represent the interface, Γ. We set the appropriate forcing term $\mathbf{f}_S$ and the source g_D, such that the following solution to the Stokes-Darcy coupled problem, with $\mathbf{f}_D=\mathbf{0}$, is exact

$$\mathbf{u}_S(x,y)=\begin{pmatrix}-4(x^2-1)^2(y^2-1)y\\ 4(x^2-1)(y^2-1)^2x\end{pmatrix}$$

$$p_S(x,y)=-sin(x)e^y\qquad p_D(x,y)=-sin(x)e^y.$$

In this first example it is satisfied that $\mathbf{u}_S=0$ in Γ_S and the two boundary conditions on the interface are nonhomogeneous. These example were also studied in [23] where the authors apply Raviart-Thomas elements of lowest order and piecewise constants for the velocities and pressures in both domains, and in [4] where the authors apply the classical Mini-element to the coupled Stokes-Darcy problem.

Figures 4-6 and 7 show, respectively, the approximate and exact velocities and the approximate and exact values of the pressures for the Stokes region, while Figures 8-10 and 11 display the corresponding for the Darcy region. Tables 1 and 2 show that optimal rate of convergence can be also reached with our method for a set of shape-regular triangulations of the domain $\overline{\Omega}_S\cup\overline{\Omega}_D$.

We look at the efficiency of the method in approximating the velocities and the pressures.

h	$e_0(p_S)$	$r_0(p_S)$	$e_0(p_D)$	$r_0(p_D)$
0.0884	0.00061	3.16209	0.00023	2.00030
0.0442	0.00010	2.58392	0.00005	1.99902
0.0221	0.00002	2.14321	0.00001	1.99948

TABLE 1. Mesh-sizes, errors, and rates of convergence (Example 1)

Second example : Let $\Omega_D=\Big\{(x,y)\in\mathbb{R}^2:\ \text{if } x\in(0,\frac{1}{2}),0<y<\frac{1}{2}x+\frac{1}{2}\text{ and if } x\in[\frac{1}{2},1),0<y<-\frac{1}{2}x+1\Big\}$ and $\Omega_S=(0,1)\times(0,1)\setminus\Omega_D$ (see Figure 12). Note that the

h	$e_0(\text{div } \mathbf{v}_S)$	$r_0(\text{div } \mathbf{v}_S)$	$e_0(\text{div } \mathbf{v}_D)$	$r_0(\text{div } \mathbf{v}_D)$	$e_1(\mathbf{v}_S)$	$r_1(\mathbf{v}_S)$
0.0884	0.01102	1.99218	0.00014	2.17030	0.01703	1.98998
0.0442	0.00276	1.99716	0.00003	2.03132	0.00426	1.99699
0.0221	0.00069	1.99900	0.000008	1.94426	0.00106	1.99898

TABLE 2. Mesh-sizes, errors, and rates of convergence (Example 1)

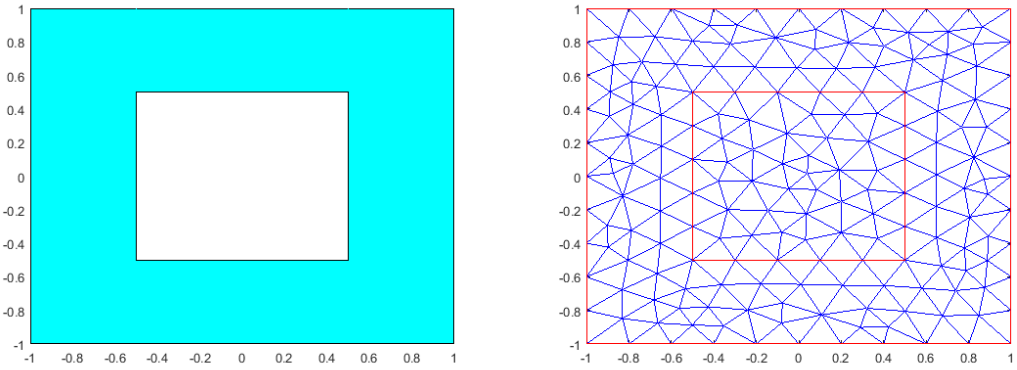

FIGURE 3. Full polygonal domain (Example 1)

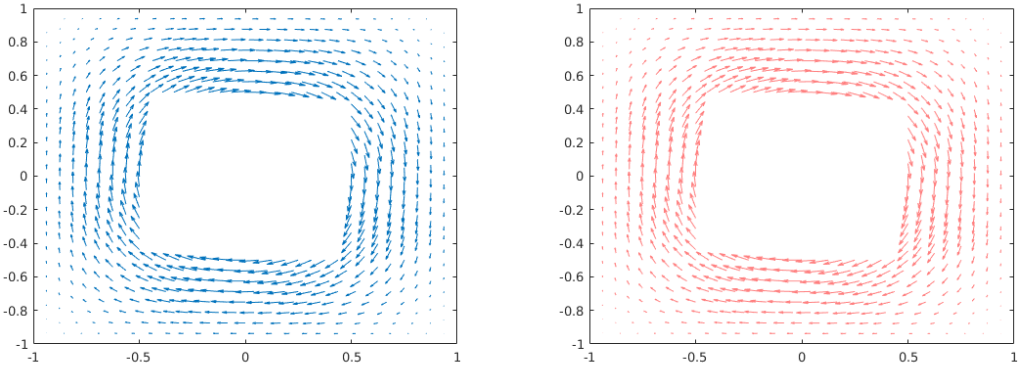

FIGURE 4. Vector charts $\mathbf{u}_S$ and $\mathbf{u}_{S,h}$ (Example 1)

interface turns out to be a union of two segments, i.e., $\Gamma = \{(x,y) \in \mathbb{R}^2 : \text{ for } x \in (0, \frac{1}{2}), y = \frac{1}{2}x + \frac{1}{2} \text{ and } \text{ for } x \in [\frac{1}{2}, 1), y = -\frac{1}{2}x + 1\}$.

We select the right-hand terms $\mathbf{f}_S$, g_S, $\mathbf{f}_D$, g_D and the boundary conditions according to the analytical solution given by

$$\mathbf{u}_S(x,y) = \begin{pmatrix} (1-x)x(1-y)(y+\frac{1}{2}x-1) \\ \frac{1}{2}(1-x)x(1-y)(y+\frac{1}{2}x-1) \end{pmatrix} \quad \mathbf{u}_D(x,y) = \begin{pmatrix} 0 \\ y(y-\frac{1}{2}x-\frac{1}{2})(y+\frac{1}{2}-1) \end{pmatrix}$$

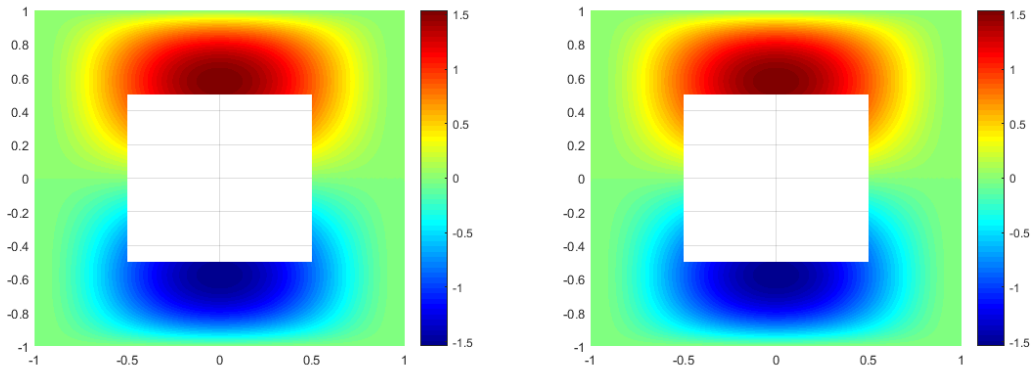

FIGURE 5. Contours of the first components of $\mathbf{u}_S$ and $\mathbf{u}_{S,h}$ (Example 1)

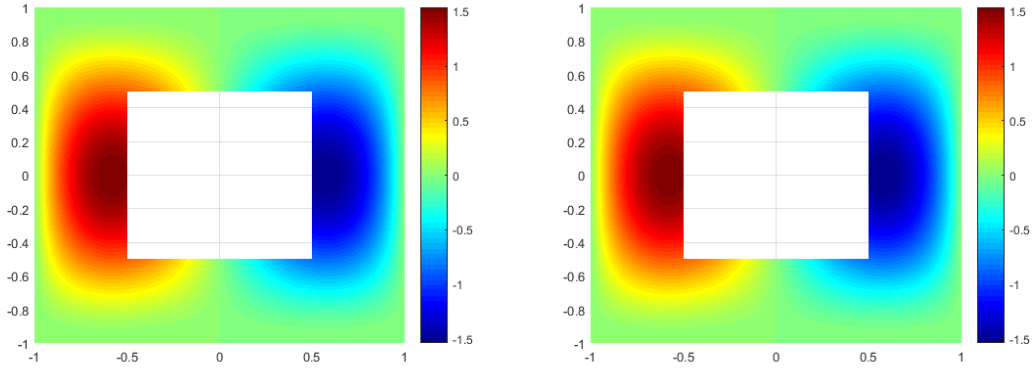

FIGURE 6. Contours of the second components of $\mathbf{u}_S$ and $\mathbf{u}_{S,h}$ (Example 1)

$$p_S(x,y) = x^3 e^y \qquad p_D(x,y) = x^3 sin(y).$$

In this second example it is satisfied that $\mathbf{u}_S = 0$ in Γ_S, $\mathbf{u}_D \cdot \boldsymbol{n_D} = 0$ in Γ_D and the two boundary conditions on the interface are nonhomogeneous.

Figures 13-15 and 16 show, respectively, the approximate and exact velocities and the approximate and exact values of the pressures for the Stokes region, while Figures 17-19 and 20 display the corresponding for the Darcy region. The obtained errors and estimated rate of convergence are given in Table 3 and in Table 4. The numerical results also suggest that this formulation is stable and that the optimal order of convergence is reached.

Third example : Let $\Omega_S = (0, \frac{1}{2}) \times (0, \frac{1}{2})$, $\Omega_D = (0, \frac{1}{2}) \times (-\frac{1}{2}, 0)$ and $\Gamma = (0, \frac{1}{2}) \times \{0\}$ (see Figure 21). We select the right-hand terms $\mathbf{f}_S$, g_S, $\mathbf{f}_D$, g_D and the boundary conditions according to the analytical solution given by

$$\mathbf{u}_S(x,y) = \mathbf{u}_D(x,y) = \begin{pmatrix} -xcos(\pi x)sin(\pi y) \\ -\frac{2}{\pi}cos(\pi x)cos(\pi y) + xsin(\pi x)cos(\pi y) \end{pmatrix}$$

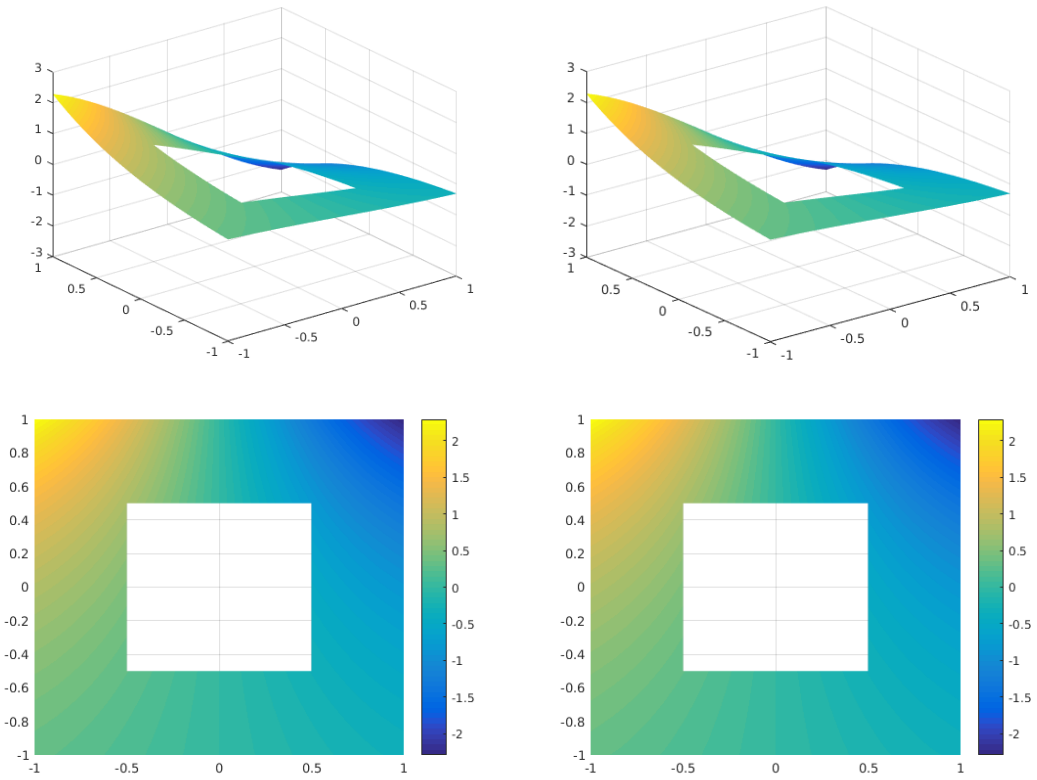

FIGURE 7. p_S and $p_{S,h}$, pressure figures (above) and pressure contours (bellow) (Example 1)

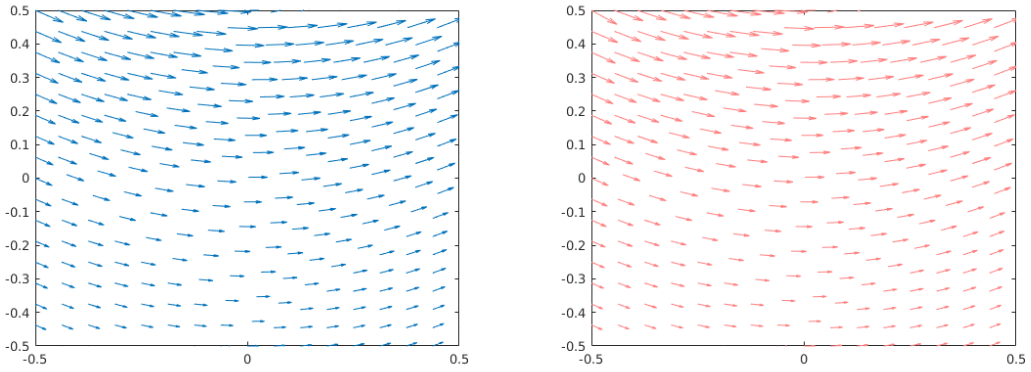

FIGURE 8. Vector charts $\mathbf{u}_D$ and $\mathbf{u}_{D,h}$ (Example 1)

$$p_S(x,y) = p_D(x,y) = sin(\pi y)\big[-cos(\pi x) + 2\pi x sin(\pi x)\big] + 4xe^{-4x}cos(\pi y) - \frac{2}{\pi}\big(1 - 5e^{-2}\big).$$

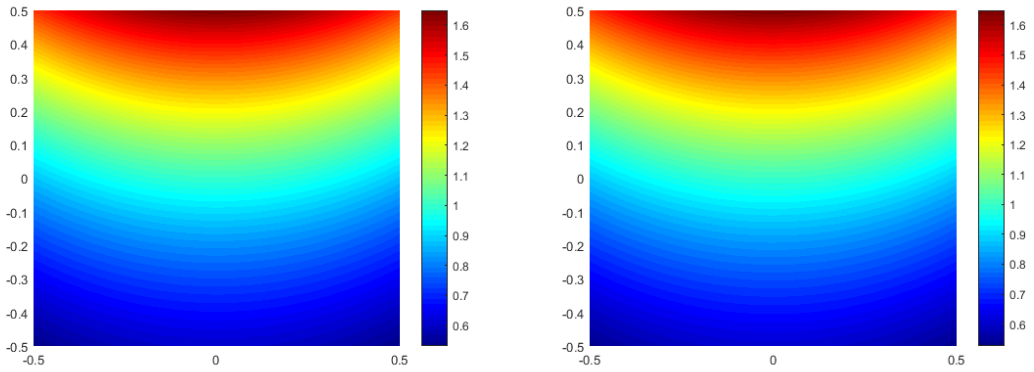

FIGURE 9. Contours of the first components of $\mathbf{u}_D$ and $\mathbf{u}_{D,h}$ (Example 1)

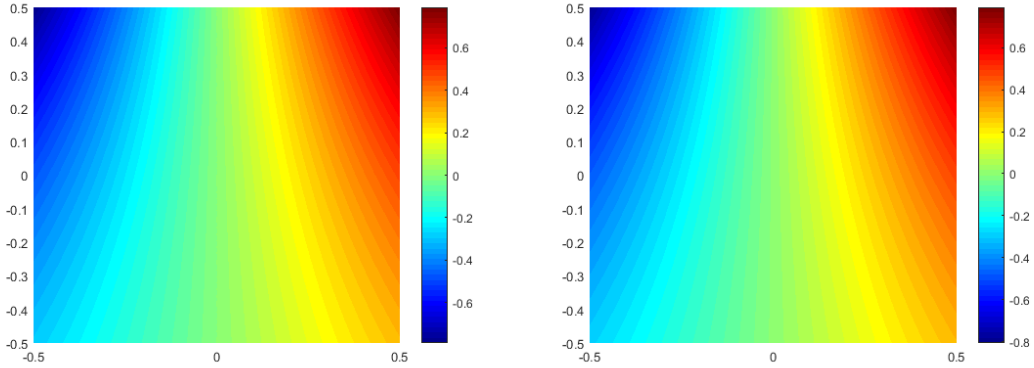

FIGURE 10. Contours of the second components of $\mathbf{u}_D$ and $\mathbf{u}_{D,h}$ (Example 1)

h	$e_0(p_S)$	$r_0(p_S)$	$e_0(p_D)$	$r_0(p_D)$
0.1250	0.00094	1.96518	0.00081	1.94438
0.0625	0.00023	1.99224	0.00020	1.98862
0.0313	0.00005	1.99989	0.00005	1.99813

TABLE 3. Mesh-sizes, errors, and rates of convergence (Example 2)

In this third example it is satisfied that $\mathbf{u}_D \cdot \boldsymbol{n}_{\boldsymbol{D}} = 0$ in Γ_D, the Dirichlet condition for the Stokes velocity on Γ_S and the two boundary conditions on the interface are nonhomogeneous.

These example were also studied in [20] where the author apply Taylor-Hood $\mathbf{P}_2 - P_1$ elements for approximating $(\mathbf{u}_S, p_S)$, Raviart-Thomas $\mathbf{RT}_1 - discP_1$ elements for approximating $(\mathbf{u}_D, p_D)$ and P_1 elements for approximating the interface pressure λ. The author also used other combinations of elements for the same example:

(1) $\mathbf{P}_2 - P_1$, $\mathbf{RT}_2 - discP_2$ and P_1,

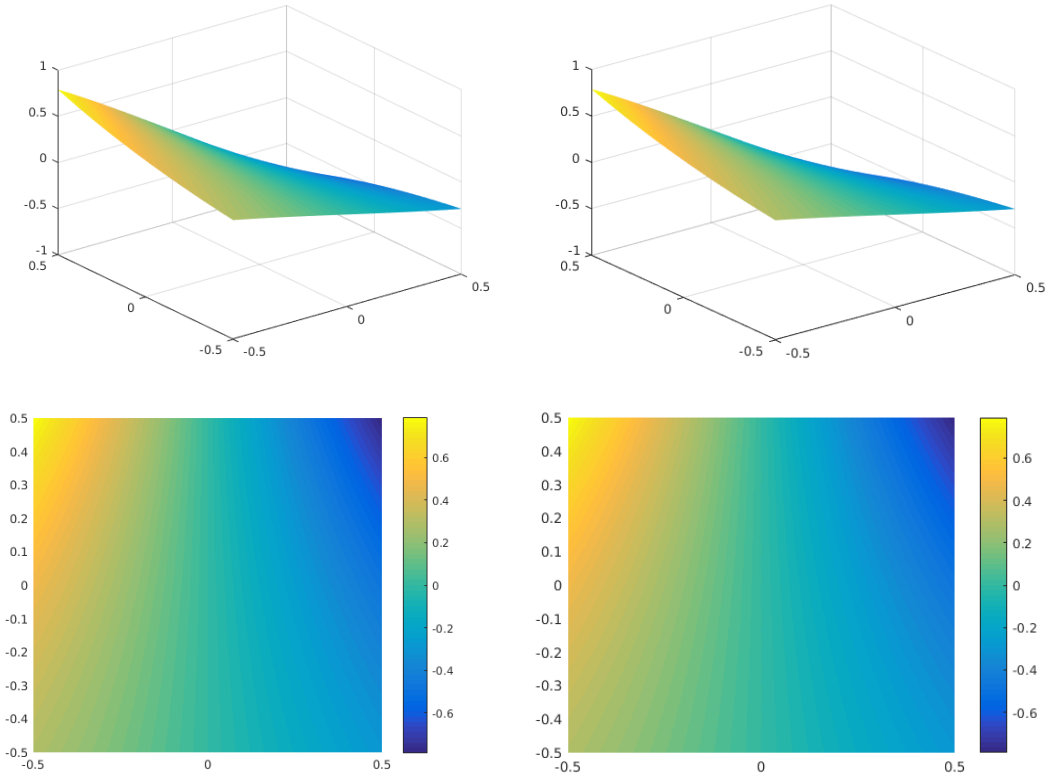

FIGURE 11. p_D and $p_{D,h}$, pressure figures (above) and pressure contours (bellow) (Example 1)

h	$e_0(\text{div } \mathbf{v}_S)$	$r_0(\text{div } \mathbf{v}_S)$	$e_0(\text{div } \mathbf{v}_D)$	$r_0(\text{div } \mathbf{v}_D)$	$e_1(\mathbf{v}_S)$	$r_1(\mathbf{v}_S)$
0.1250	0.00054	1.97506	0.00252	2.01308	0.00063	1.99574
0.0625	0.00013	2.00516	0.00062	2.01810	0.00015	2.00575
0.0313	0.00003	2.00748	0.00015	2.01508	0.00003	2.00547

TABLE 4. Mesh-sizes, errors, and rates of convergence (Example 2)

(2) $\mathbf{P}_2 - P_1$, $\mathbf{RT}_2 - discP_2$ and P_2,
(3) $(\mathbf{P}_1 \oplus \mathbf{Bubble}) - P_1$, $\mathbf{RT}_1 - discP_1$ and P_1.

Figures 22-24 and 25 show, respectively, the approximate and exact velocities and the approximate and exact values of the pressures for the Stokes region, while Figures 26-28 and 29 display the corresponding for the Darcy region. The obtained errors and estimated rate of convergence are given in Table 5 and in Table 6.

We emphasize that the numerical results confirm the good performance of the mixed finite element scheme with Taylor-Hood elements for the Stokes-Darcy coupled problem.

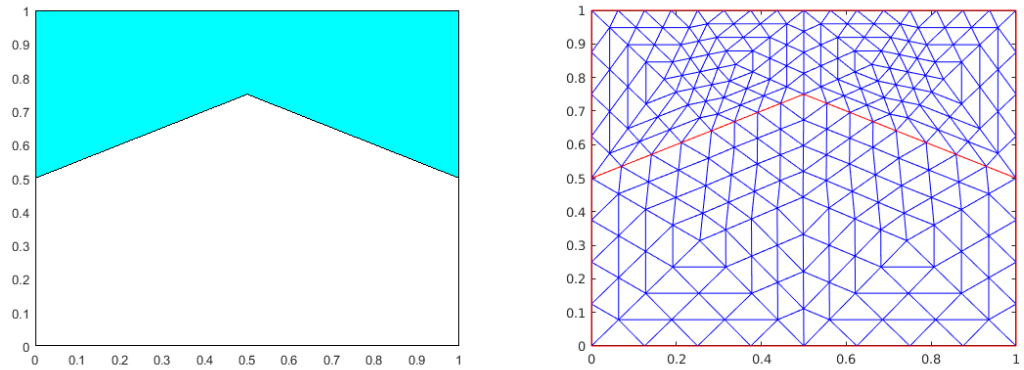

FIGURE 12. Full polygonal domain (Example 2)

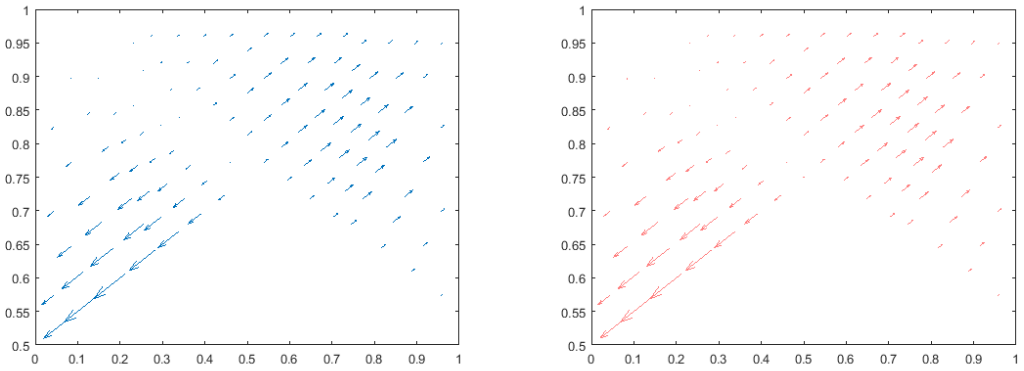

FIGURE 13. Vector charts $\mathbf{u}_S$ and $\mathbf{u}_{S,h}$ (Example 2)

h	$e_0(p_S)$	$r_0(p_S)$	$e_0(p_D)$	$r_0(p_D)$
0.03125	0.00052	2.01299	0.00055	2.01057
0.01562	0.00013	2.00506	0.00013	2.00516
0.00781	0.00003	2.00213	0.00003	2.00247

TABLE 5. Mesh-sizes, errors, and rates of convergence (Example 3)

This work was partially supported by ANPCyT under grant PICT 2018-3017, CONICET under grant PIP (2014-2016) 11220130100184CO and by Universidad de Buenos Aires under grant 20020170100056BA.

REFERENCES

[1] R. Araya, G. R. Barrenechea and A. Poza, *An adaptive stabilized finite element method for the generalized Stokes problem*, Journal of Computational and Applied Mathematics. 214 (2008) pp. 457-479.

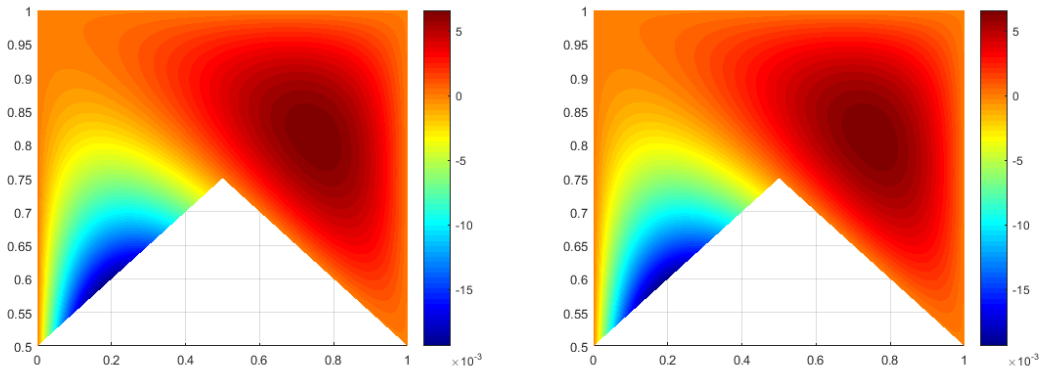

FIGURE 14. Contours of the first components of $\mathbf{u}_S$ and $\mathbf{u}_{S,h}$ (Example 2)

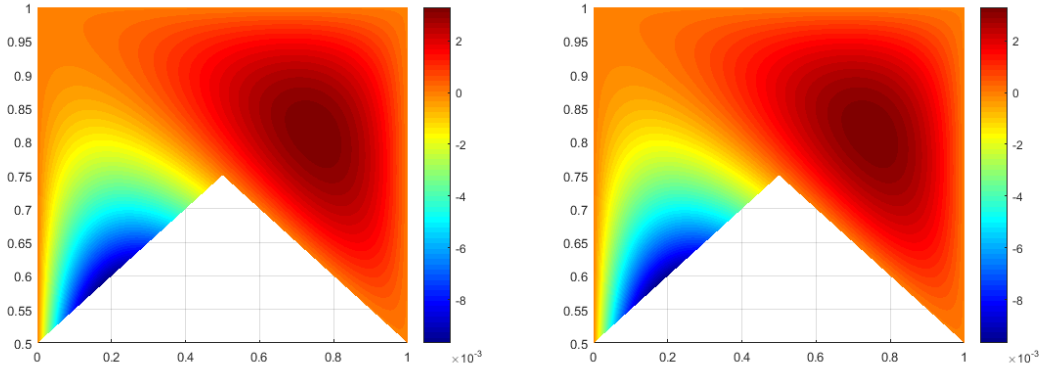

FIGURE 15. Contours of the second components of $\mathbf{u}_S$ and $\mathbf{u}_{S,h}$ (Example 2)

h	$e_0(\text{div } \mathbf{v}_S)$	$r_0(\text{div } \mathbf{v}_S)$	$e_0(\text{div } \mathbf{v}_D)$	$r_0(\text{div } \mathbf{v}_D)$	$e_1(\mathbf{v}_S)$	$r_1(\mathbf{v}_S)$
0.03125	0.00024	2.03288	0.00031	2.08003	0.00071	1.99647
0.01562	0.00006	2.01448	0.00007	2.03863	0.00017	1.99814
0.00781	0.00001	2.00667	0.00001	2.01812	0.00004	1.99904

TABLE 6. Mesh-sizes, errors, and rates of convergence (Example 3)

[2] M. G. Armentano, *Stabilization of low-order cross-grid P_kQ_l mixed finite elements*, Journal of Computational and Applied Mathematics, 330 (2018) pp. 340-355.

[3] M. G. Armentano and J. Blasco, *Stable and unstable cross-grid P_kQ_l mixed finite elements for the Stokes problem*, Journal of Computational and Applied Mathematics. 234 (5), (2010) pp. 1404-1416.

[4] M. G. Armentano and M. L. Stockdale, *A unified mixed finite element approximations of the Stokes-Darcy coupled problem*, Computers and Mathematics with Applications 77 (9), (2019) pp. 2568-2584.

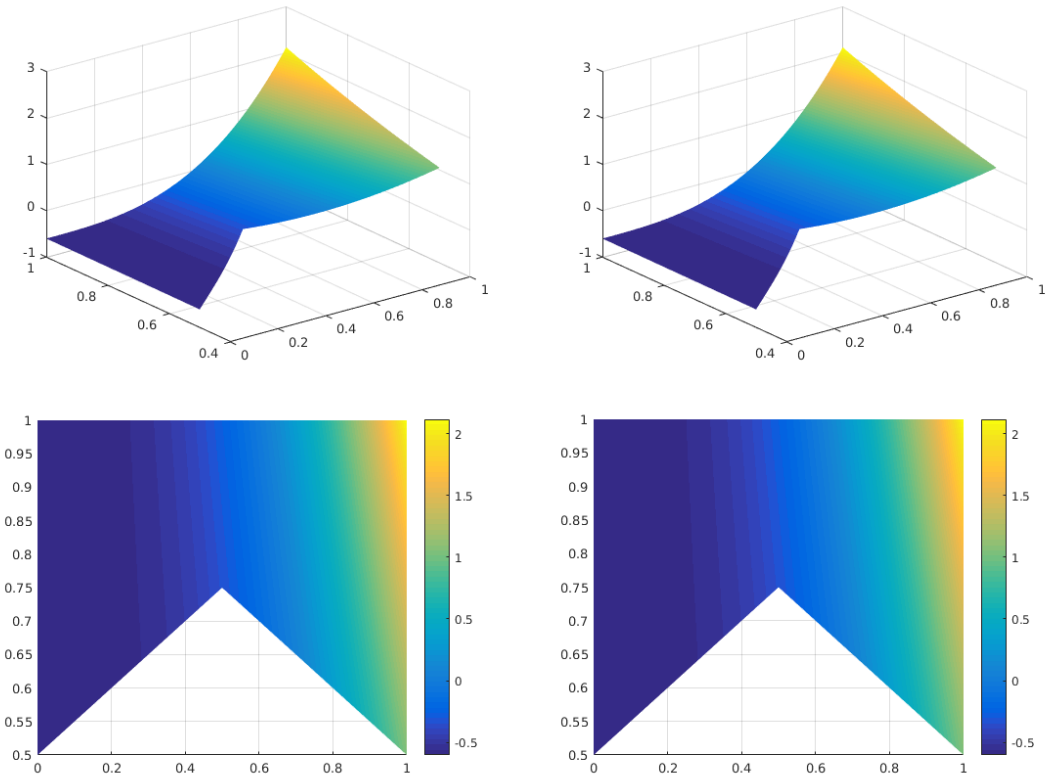

FIGURE 16. p_S and $p_{S,h}$, pressure figures (above) and pressure contours (bellow) (Example 2)

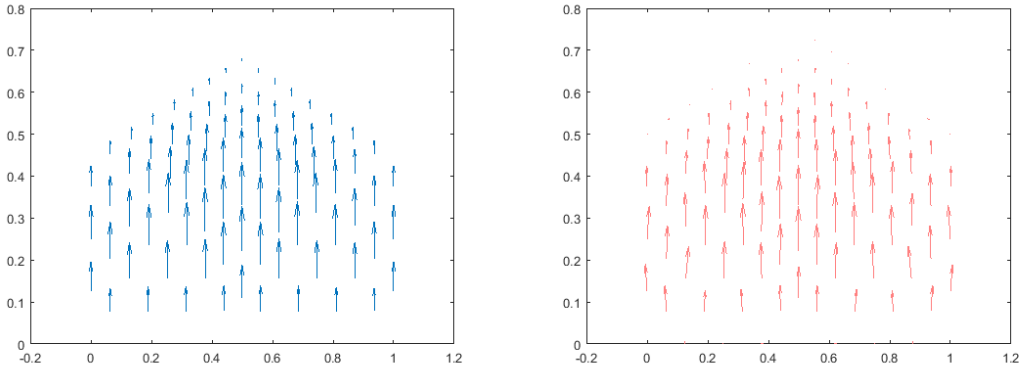

FIGURE 17. Vector charts $\mathbf{u}_S$ and $\mathbf{u}_{S,h}$ (Example 2)

[5] M. G. Armentano and M. L. Stockdale, *Approxinations by mini mixed finite element for the Stokes-Darcy coupled problem on curved domains*, International Journal of Numerical Analysis and Modeling, 18 (2), (2021) pp. 203-234.

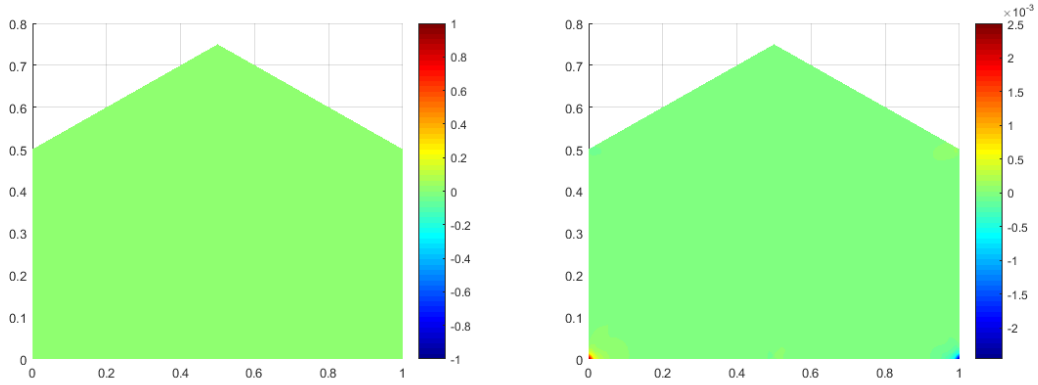

FIGURE 18. Contours of the first components of $\mathbf{u}_D$ and $\mathbf{u}_{D,h}$ (Example 2)

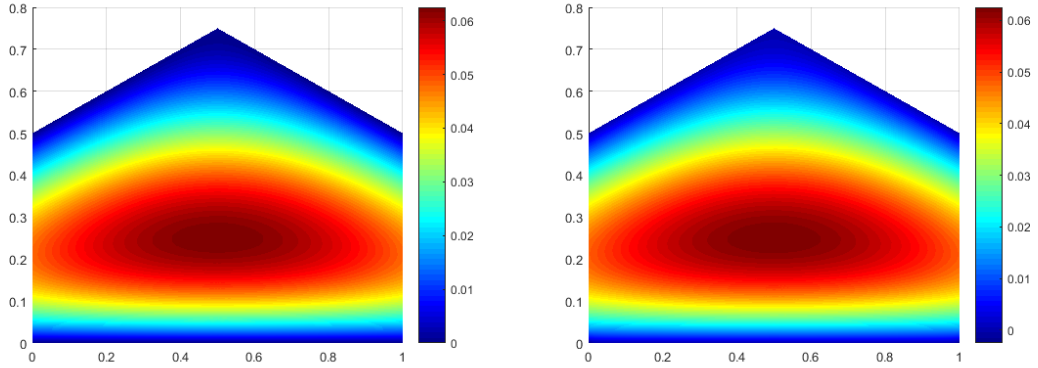

FIGURE 19. Contours of the second components of $\mathbf{u}_D$ and $\mathbf{u}_{D,h}$ (Example 2)

[6] D. N. Arnold, F. Brezzi and M. Fortin, *A stable finite element for the Stokes equations*, Calcolo 21 (1984) pp. 337-344.

[7] S. Badia and R. Codina, *Stokes, Maxwell and Darcy: A single finite element approximation for three model problems*, Applied Numerical Mathematics. 62 (2012) pp. 246-263.

[8] G. R. Barrenechea, L. P. Franca and F. Valentin, *A Petrov-Galerkin enriched method: A mass conservative finite element method for the Darcy equation*, Comput. Methods Appl. Mech. Engrg. 196 (2007) pp. 2449-2464.

[9] G. Beavers and D. Joseph, *Boundary conditions at a naturally impermeable wall*, Journal of Fluid Mechanics 30 (1967) pp. 197-207.

[10] P. B. Bochev and C. R. Dohrmann, *A computational study of stabilized, low-order C0 finite element approximations of Darcy equations*, Comput. Mech. 38 (2006) pp. 323-333.

[11] P. B. Bochev, C. R. Dohrmann, M. D. Gunzburger, *Stabilization of low-order mixed finite elements for the Stokes equations*, SIAM J. Numer. Anal. 44 (1) (2006) pp. 82-101.

[12] D. Boffi, *Minimal stabilizations of the P_{k+1}-P_k approximation of the stationary Stokes equations*, Mathematical Models & Methods in Applied Sciences 5 (2) (1995) pp. 213-224.

[13] D. Boffi, F. Brezzi, L. Demkowicz, R. G. Durán, R. Falk and M. Fortin, *Mixed Finite Elements, Compatibility Conditions, and Applications*, Lectures Notes in Mathematics, 1939, 2008.

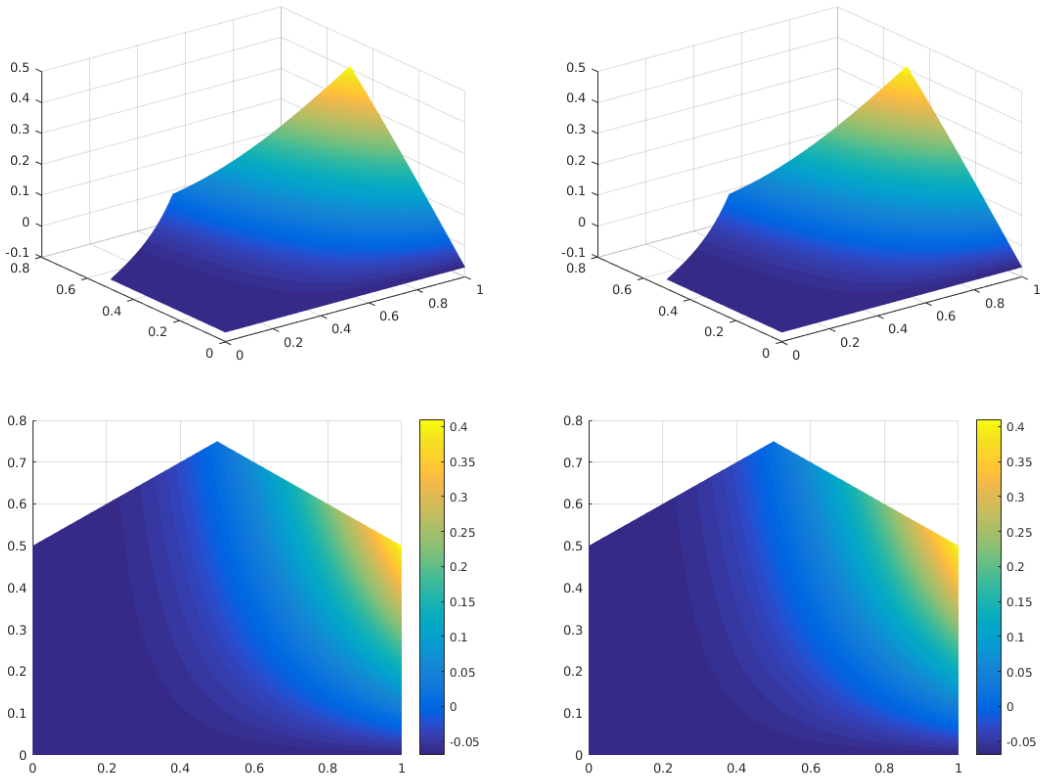

FIGURE 20. p_D and $p_{D,h}$, pressure figures (above) ans pressure contours (bellow) (Example 2)

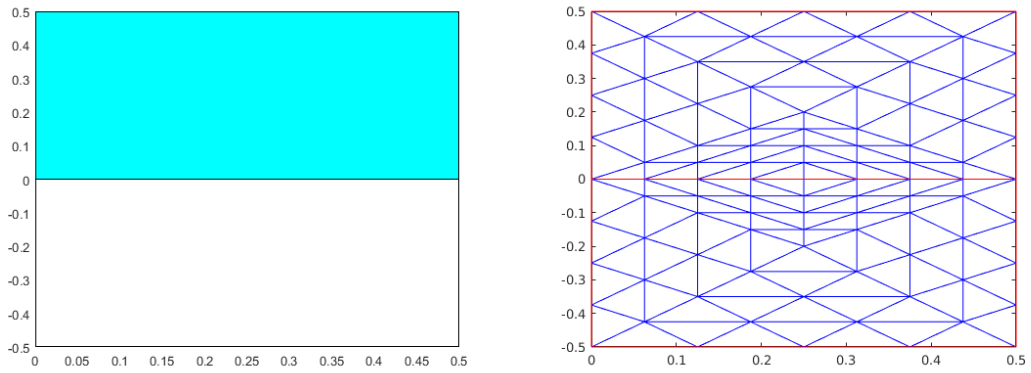

FIGURE 21. Full polygonal domain (Example 3)

[14] D. Boffi and L. Gastaldi, *On the quadrilateral Q_2-P_1 element for the Stokes problem*, International Journal for Numerical Methods in Fluids, 39 (4)(2002) pp. 1001-1011.

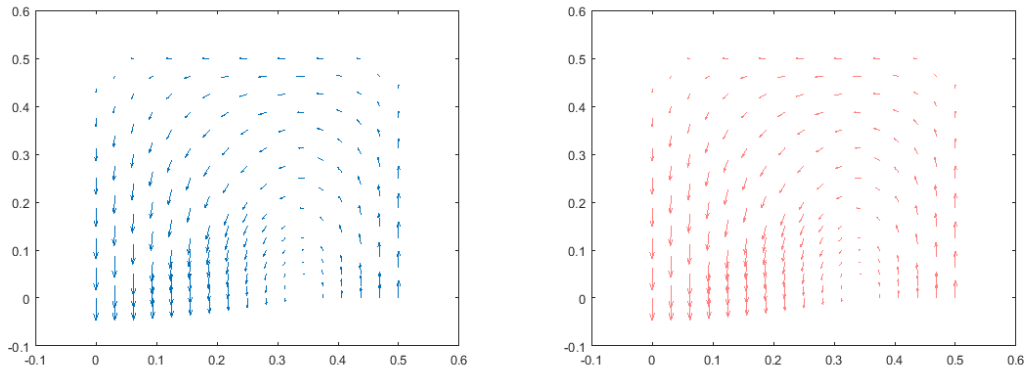

FIGURE 22. Vector charts $\mathbf{u}_S$ and $\mathbf{u}_{S,h}$ (Example 3)

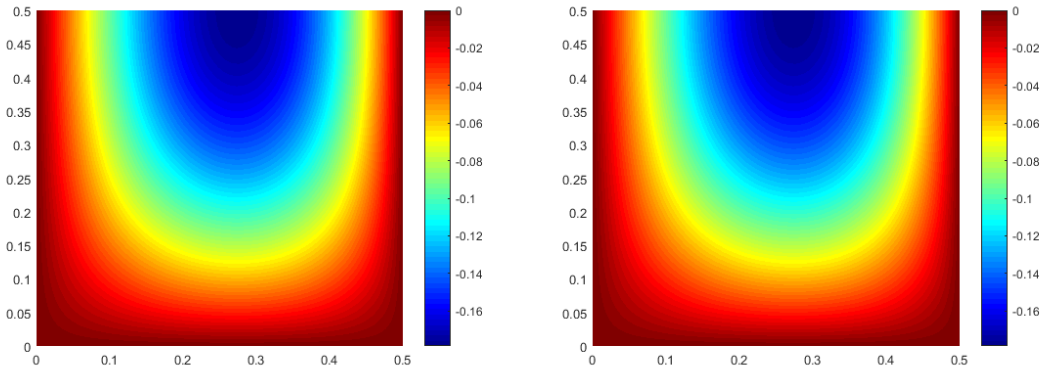

FIGURE 23. Contours of the first components of $\mathbf{u}_S$ and $\mathbf{u}_{S,h}$ (Example 3)

[15] D. Braess, *Finite elements: Theory, fast solvers, and applications in solid mechanics*, Cambridge University Press, 2007.

[16] F. Brezzi and R. Falk, *Stability of higher-order Hood-Taylor methods*, SIAM Journal on Numerical Analysis 28 (3) (1991) pp. 581-590.

[17] F. Brezzi and M. Fortin, *Mixed and Hybrid Finite Element Methods*, Springer, Berlin Heidelberg New York, 1991.

[18] Long Chen, *A simple construction of a Fortin operator for the two dimensional TaylorHood element*, Computers and Mathematics with Applications. 68 (10) (2014) pp. 1368-1373

[19] M. Discacciati ans A. Quarteroni, *NavierStokes/Darcy coupling: modeling, analysis, and numerical approximation*, Rev. Math. Comput. 22 (2009) pp. 315-426.

[20] V. J. Ervin, *Approximation of coupled Stokes-Darcy flow in an axisymmetric domain* Comput. Methods Appl. Mech. Engrg. 258 (2013) pp. 96108.

[21] R. Falk *A Fortin Operator for two-dimensional Taylor-Hood elements*, ESAIM: M2AN 42 (2008) pp. 411-424.

[22] G. N. Gatica, S. Meddahi and R. Oyarzúa, *A conforming mixed finite-element method for the coupling of fluid flow with porous media flow*, IMA Journal of Numerical Analysis, 29 (2009) pp. 86-108.

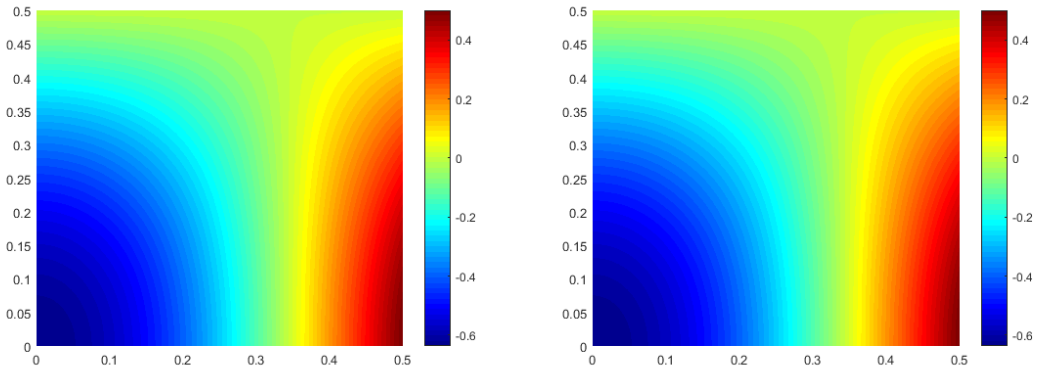

FIGURE 24. Contours of the second components of $\mathbf{u}_S$ and $\mathbf{u}_{S,h}$ (Example 3)

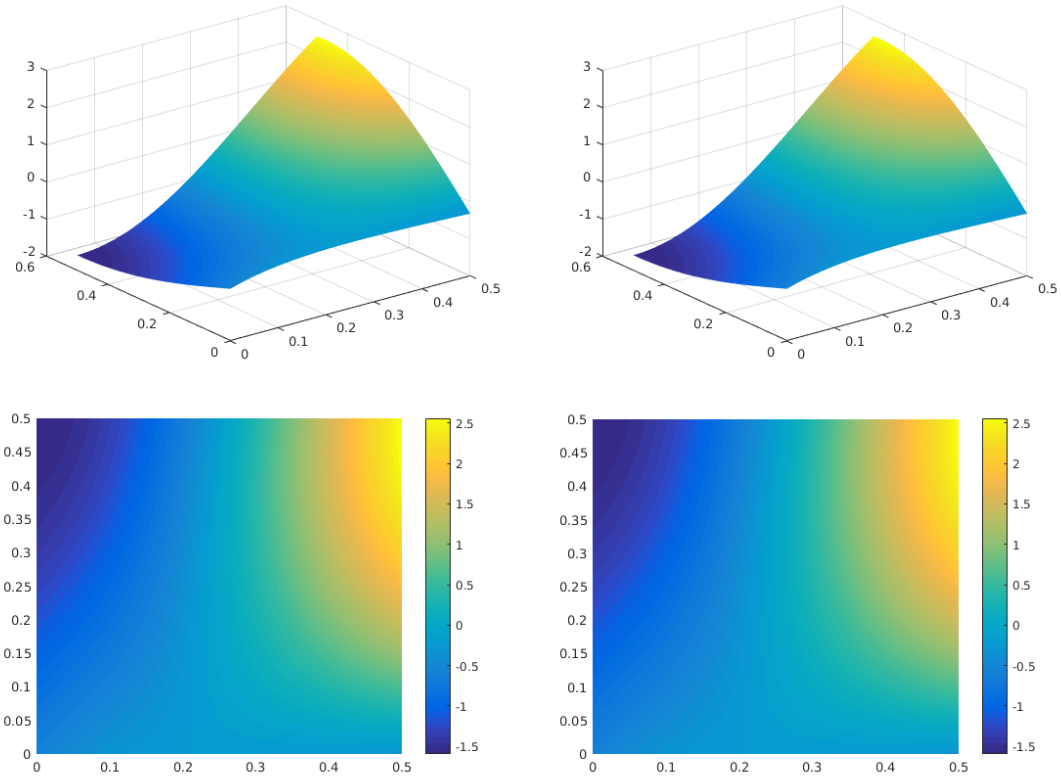

FIGURE 25. p_S and $p_{S,h}$, pressure figures (above) and pressure contours (bellow) (Example 3)

[23] G. N. Gatica, R. Oyarzúa and F. J. Sayas, *Analysis of fully-mixed finite element methods for the Stokes-Darcy coupled problem*, Mathematics of Computation Vol. 80, Number 276 (2011) pp. 1911-1948.

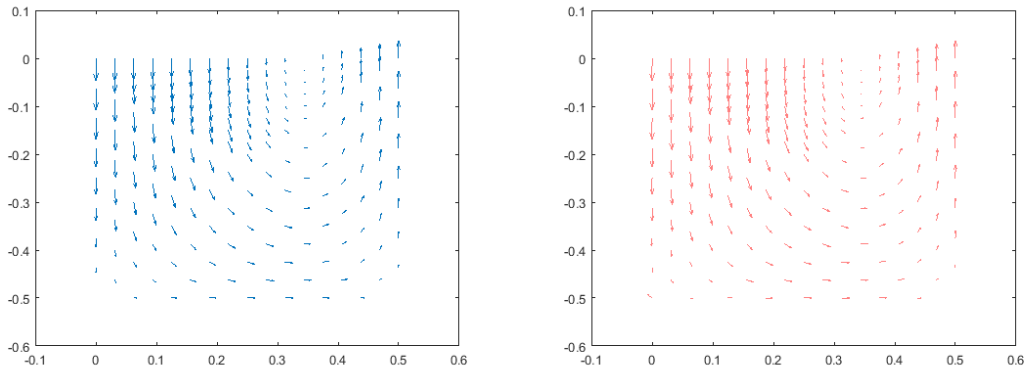

FIGURE 26. Vector charts $\mathbf{u}_S$ and $\mathbf{u}_{S,h}$ (Example 3)

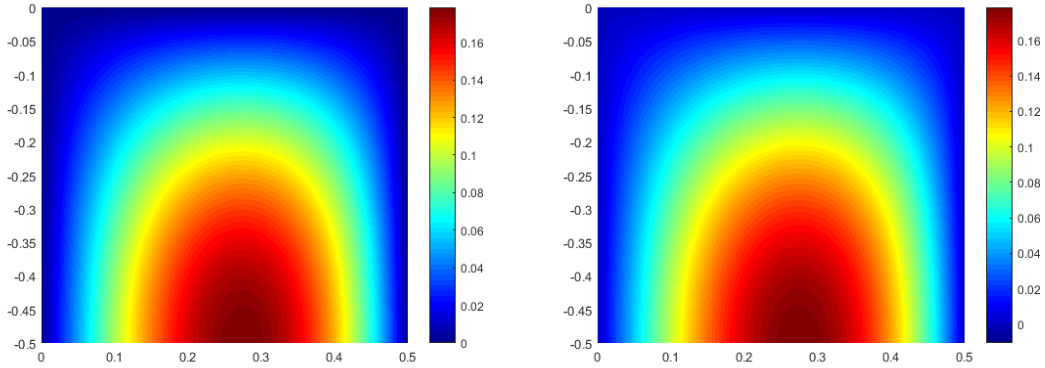

FIGURE 27. Contours of the first components of $\mathbf{u}_D$ and $\mathbf{u}_{D,h}$ (Example 3)

[24] G. N. Gatica, R. Ruiz-Baier and G. Tierra, Giordano, *A mixed finite element method for Darcy's equations with pressure dependent porosity*, Math. Comp. 85 (297) (2016) pp. 133.

[25] V. Girault and P. A. Raviart, *Finite Element Methods for Navier-Stokes Equations. Theory and Algorithms*, Springer Series in Computational Mathematics, Vol. 5, Springer-Verlag, 1986.

[26] P. Hood and C. Taylor,*Numerical solution of the NavierStokes equations using the finite element technique.* Comput. Fluids, 1, (1973) pp. 1-28.

[27] T. Karper, K. A. Mardal and R. Winther, *Unified Finite Element Discretizations Of Coupled Darcy-Stokes Flow*, Numerical Methods for Partial Differential Equations. 25 (2) (2009) pp. 311-326.

[28] W. J. Layton, F. Schieweck and I. Yotov, *Coupling fluid flow with porous media flow*, Siam J. Numer. Anal., 40 (6) (2003) pp. 2195-2218.

[29] K-A. Mardal, J. Schberl and R. Winther, *A uniformly stable Fortin operator for the TaylorHood element*, Numerische Mathematik 123 (2013) pp. 537-551

[30] N. S. Nicaise, B. Ahounou and W. Houedanou, *Residual-based a posteriori error estimates for a nonconforming finite element discretization of the Stokes-Darcy coupled problem: isotropic discretization*, Afr. Mat. 27, No. 3-4 (2016) pp. 701729.

[31] H. Rui and R. Zhang, *A unified stabilized mixed finite element method for coupling Stokes and Darcy flows*, Comput. Methods Appl. Mech. Eng. 198 (2009) pp. 2692-2699.

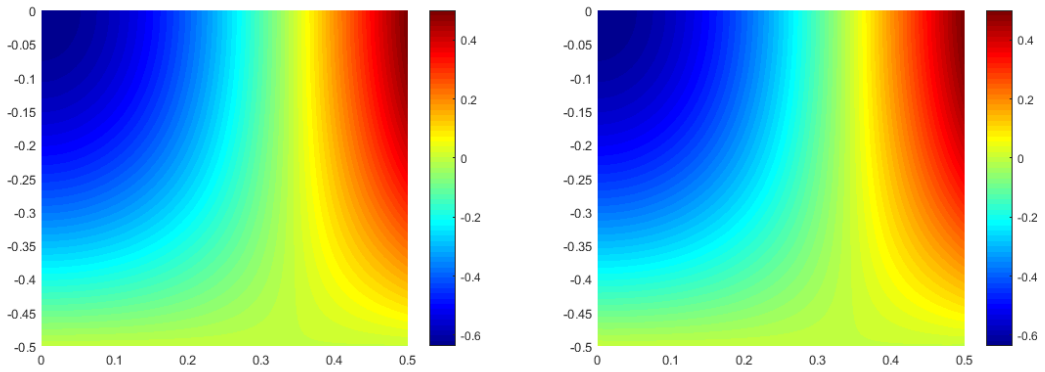

FIGURE 28. Contours of the second components of $\mathbf{u}_D$ and $\mathbf{u}_{D,h}$ (Example 3)

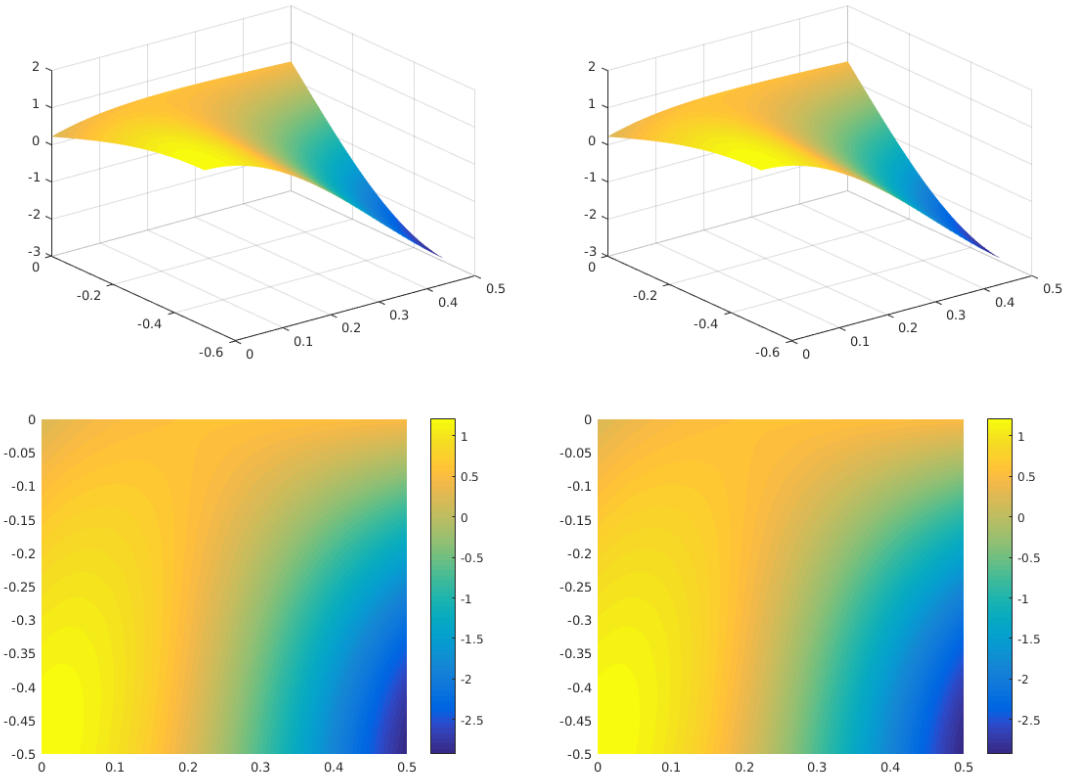

FIGURE 29. p_D and $p_{D,h}$, pressure figures (above) ans pressure contours (bellow) (Example 3)

[32] L. Ridgway Scott, *A Local Fortin Operator for Low-order Taylor-Hood Elements* preprint (2021).

[33] R. Verfürth, *A Posteriori Error Estimation Techniques for Finite Element Methods*, Numerical Mathematics and Scientific Computation, Oxford University Press, Oxford, (2013).